ENCLOSURE 12

WESTINGHOUSE REPORT WCAP-17549-NP, REVISION 0
MONTICELLO REPLACEMENT STEAM DRYER
STRUCTURAL EVALUATION FOR HIGH-CYCLE ACOUSTIC LOADS USING ACE

82 pages follow

Westinghouse Non-Proprietary Class 3

WCAP-17549-NP
Revision 0

May 2012

Monticello Replacement Steam Dryer Structural Evaluation for High-Cycle Acoustic Loads Using ACE

WCAP-17549-NP
Revision 0

Monticello Replacement Steam Dryer Structural Evaluation for High-Cycle Acoustic Loads Using ACE

Robert Theuret*
Acoustic and Structural Analysis

Gary Plonczak*
Acoustic and Structural Analysis

David Suddaby*
Acoustic and Structural Analysis

May 2012

Approved: David Forsyth*, Manager
Acoustic and Structural Analysis

*Electronically approved records are authenticated in the electronic document management system.

Westinghouse Electric Company LLC
1000 Westinghouse Drive
Cranberry Township, PA 16066

Table of Contents

LIST OF TABLES

LIST OF FIGURES

Executive Summary

A high-cycle fatigue evaluation of the Westinghouse replacement steam dryer for the Monticello plant has been completed with loads generated using acoustic circuit enhanced (ACE) Rev. 1. Acoustic loads and stresses for 98% of current licensed thermal power (CLTP) and 100% of extended power uprate (EPU) conditions have been evaluated for high-cycle fatigue and have been determined to meet the American Society of Mechanical Engineers (ASME) Boiler and Pressure Vessel (B&PV) Code Section III, Subsection NG criteria.

The results from these analyses indicate that for the Monticello replacement steam dryer at EPU operation, the minimum high-cycle fatigue stress ratio anywhere on the steam dryer is [ ]^{a,c} and occurs on the [ ]^{a,c} These results account for all the end-to-end biases and uncertainties in the loads model and finite element analysis. [

]^{a,c}.

LIST OF ABBREVIATIONS

Abbreviation	Description
ACE	acoustic circuit enhanced
ASME	American Society of Mechanical Engineers
B&PV	boiler and pressure vessel
BWR	boiling water reactor
CG	center of gravity
CLTP	current licensed thermal power
EPU	extended power uprate
FEM	finite element model
FSRF	fatigue strength reduction factor
IFT	inverse Fourier transform
MSL	main steam line
RG	Regulatory Guide
SCF	stress concentration factor
2-D	two-dimensional
3-D	three-dimensional

1 INTRODUCTION

In 2002, after increasing power to 117% of the original licensed thermal power, the steam dryer in a boiling water reactor (BWR) experienced a series of structural failures. After extensive evaluation by various industry experts, the root cause of the dryer failures was determined to be acoustic fluctuating pressure loads on the dryer, resulting from resonances produced by steam flow in the main steam lines (MSLs) across safety and relief valve inlets. The failures in the steam dryer of a BWR led to changes in Regulatory Guide (RG) 1.20, requiring plants to evaluate their steam dryer before any planned increase in power level.

The Monticello power plant has contracted Westinghouse for a replacement steam dryer and is also planning a power uprate. In conjunction with the component replacement by Monticello and the planned power uprate, an analysis has been performed to qualify the replacement steam dryer, shown in Figure 1-1, for acoustic pressure loads. The process used to perform the analysis involves [

]^{a,c} Structural qualification of the replacement dryer for the remaining duty cycle of events applicable to the Monticello operating system is documented in Reference 1.

a,c

Figure 1-1 Schematic of Monticello Replacement Steam Dryer

2 METHODOLOGY

2.1 OVERVIEW

An analysis has been performed to assess the structural integrity of the replacement dryer for the Monticello plant subject to acoustic loads. [

]^{a,c}

2.2 DESIGN REQUIREMENTS

2.2.1 [ ]^{a,c}

The replacement dryer is analyzed according to the 2004 Edition of the ASME B&PV Code, Subsection NG (Reference 2). This report documents the suitability of the replacement dryer for high-cycle fatigue loads resulting from acoustic loads. The governing criterion for the analysis is in terms of the allowable component fatigue usage. The objective of this analysis is to show that the maximum alternating stress intensity anywhere in the dryer is less than the material endurance strength at 10^{11} cycles. The applicable fatigue curve for stainless steel (the dryer is manufactured from SS316L), is shown in Figure I-9.2.2 in Appendix I of the ASME Code. The evaluation of the replacement steam dryer for non-acoustic loads is documented in Reference 1.

[

]^{a,c}.

2.2.2 Young's Modulus Correction

Before comparing the maximum alternating stress intensity to the ASME Code endurance strength, it is necessary to account for the Young's modulus correction. The analysis uses a Young's modulus of 25.425×10^6 psi, compared to the value to construct the fatigue curves of 28.3×10^6 psi. The ratio that is applied to the calculated alternating stress intensities is 1.113 (i.e. 28.3 / 25.425).

2.2.3 [ ]^{c}

[

]^{a,c}

2.3 DRYER GEOMETRY

Plots showing various aspects of the dryer configuration are provided in Figure 2-1 through Figure 2-8.

a,c

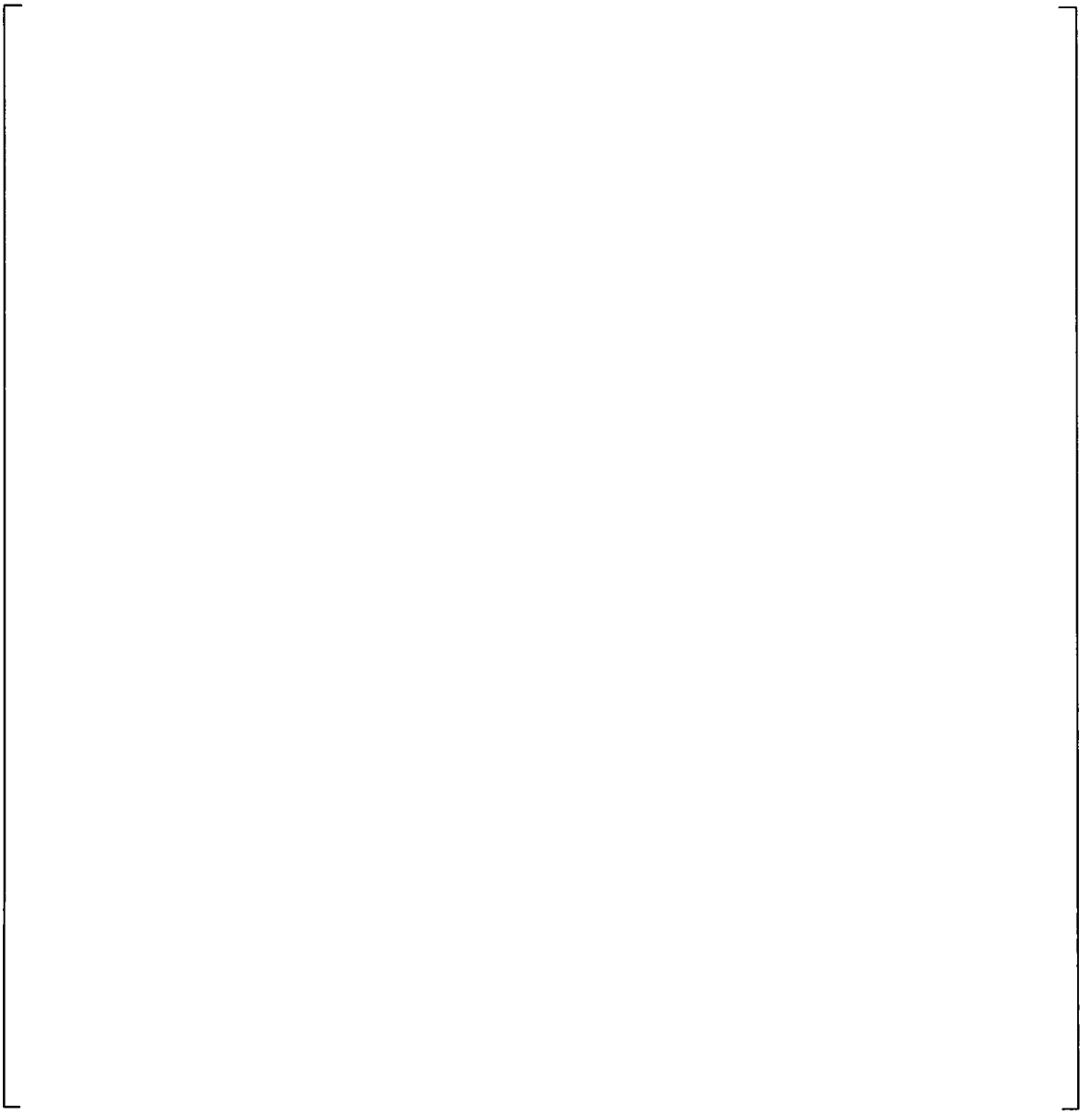

Figure 2-1 Geometry Plot: Overall Dryer

a,c

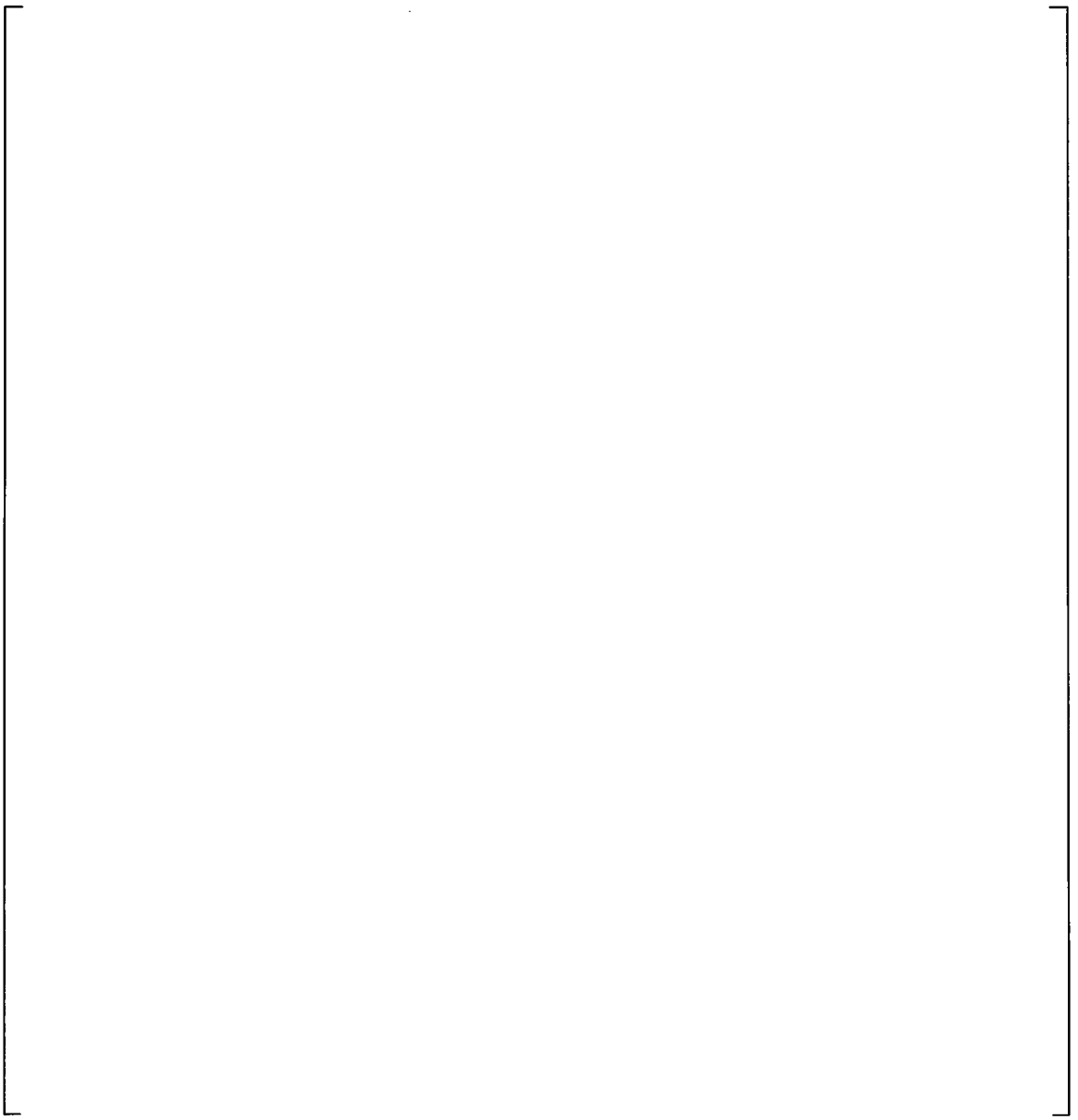

Figure 2-2 Geometry Plot: Cut-Away View

a,c

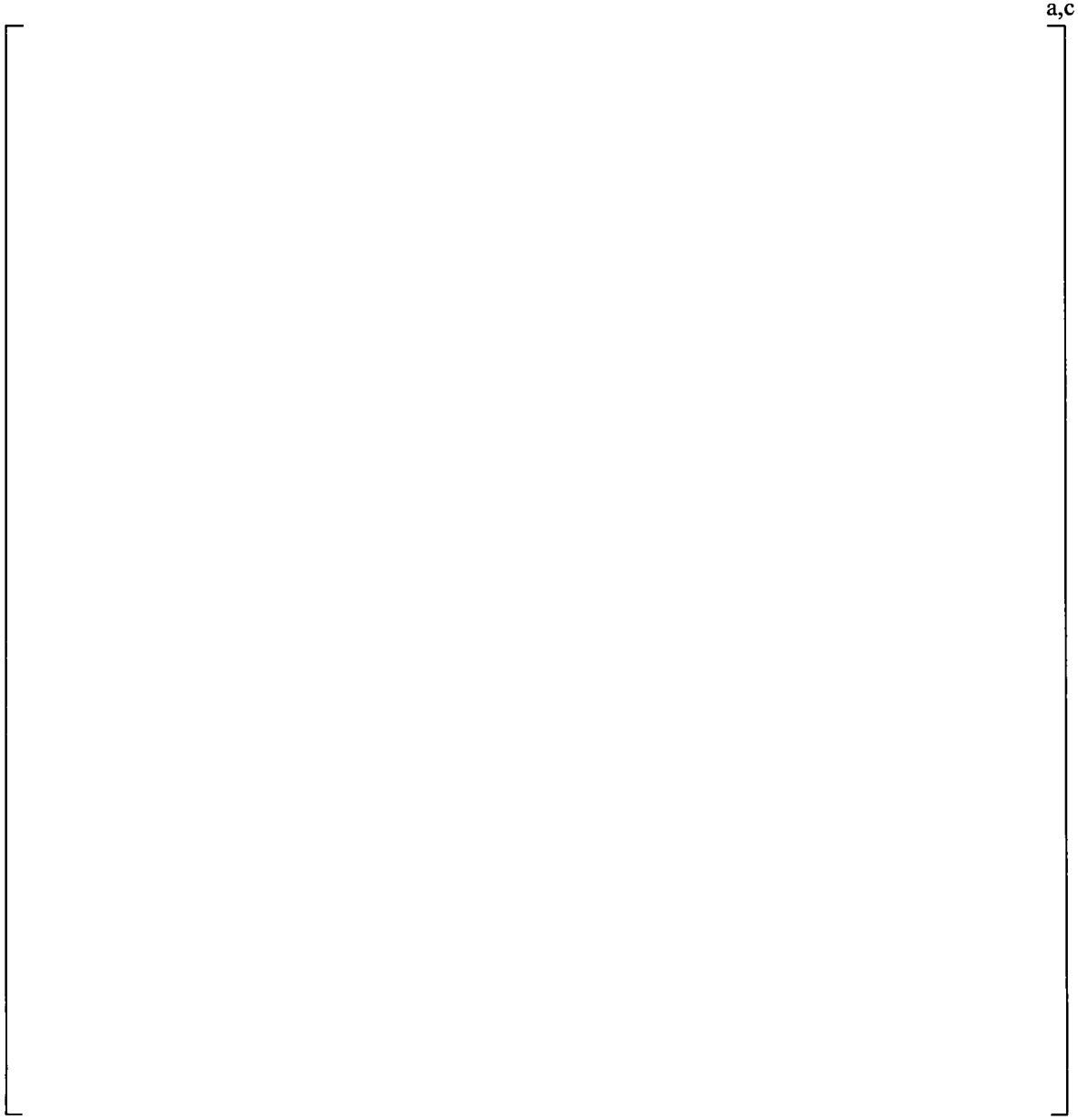

Figure 2-3 Geometry Plot: Dryer Hoods

a,c

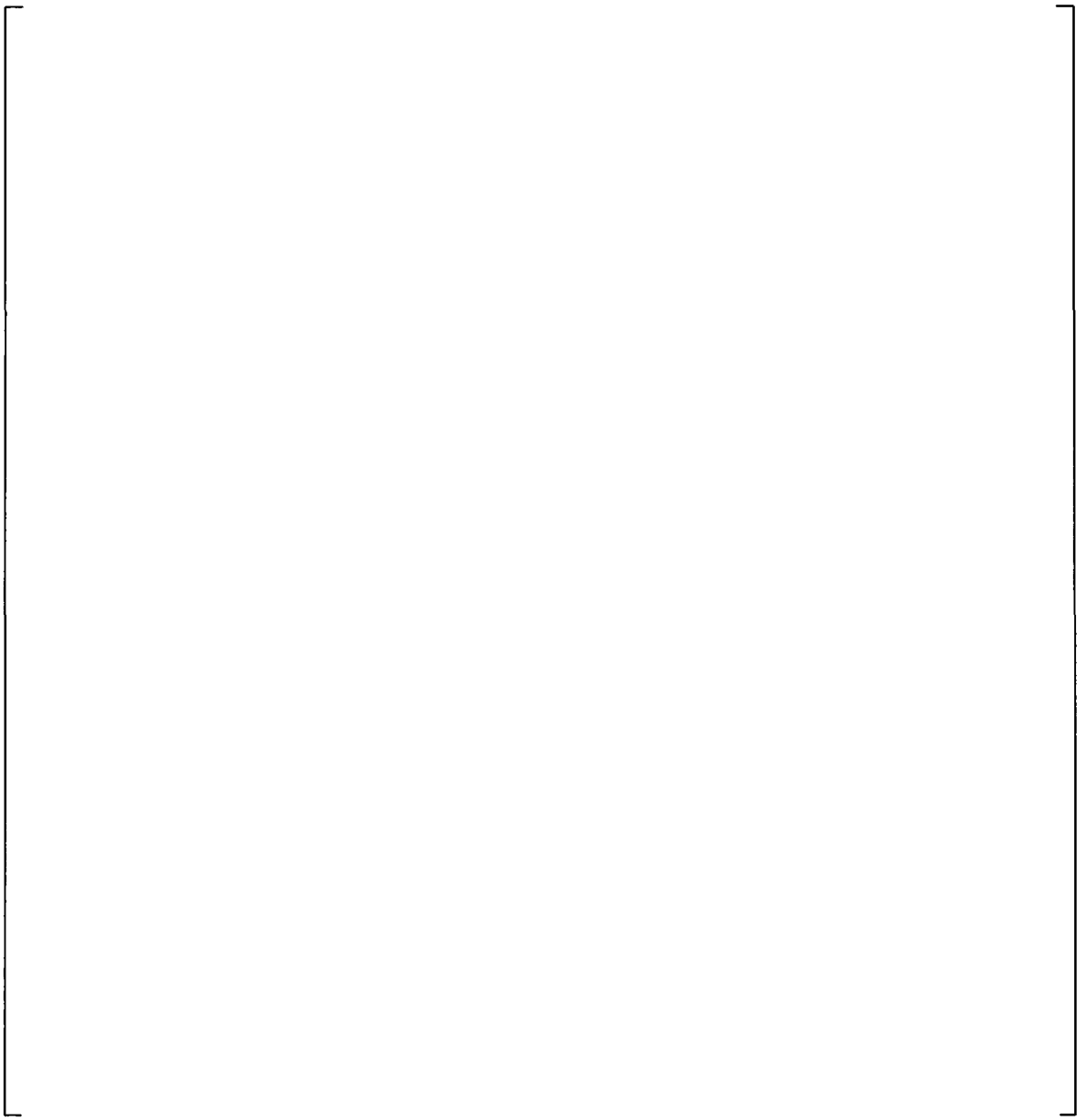

Figure 2-4 Geometry Plot: Skirt and Drain Region

a,c

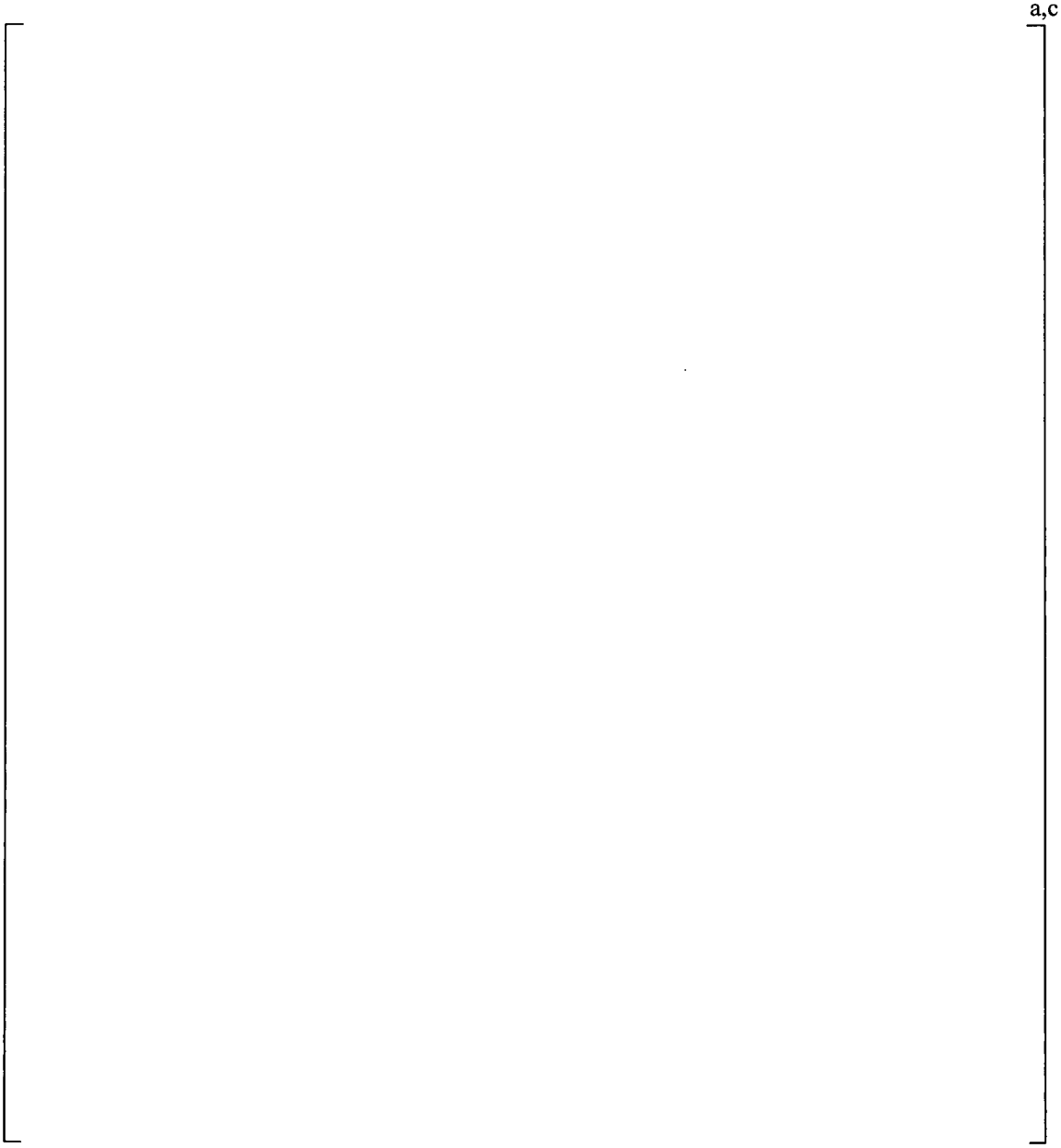

Figure 2-5 Geometry Plot: One-Eighth Sector

a,c

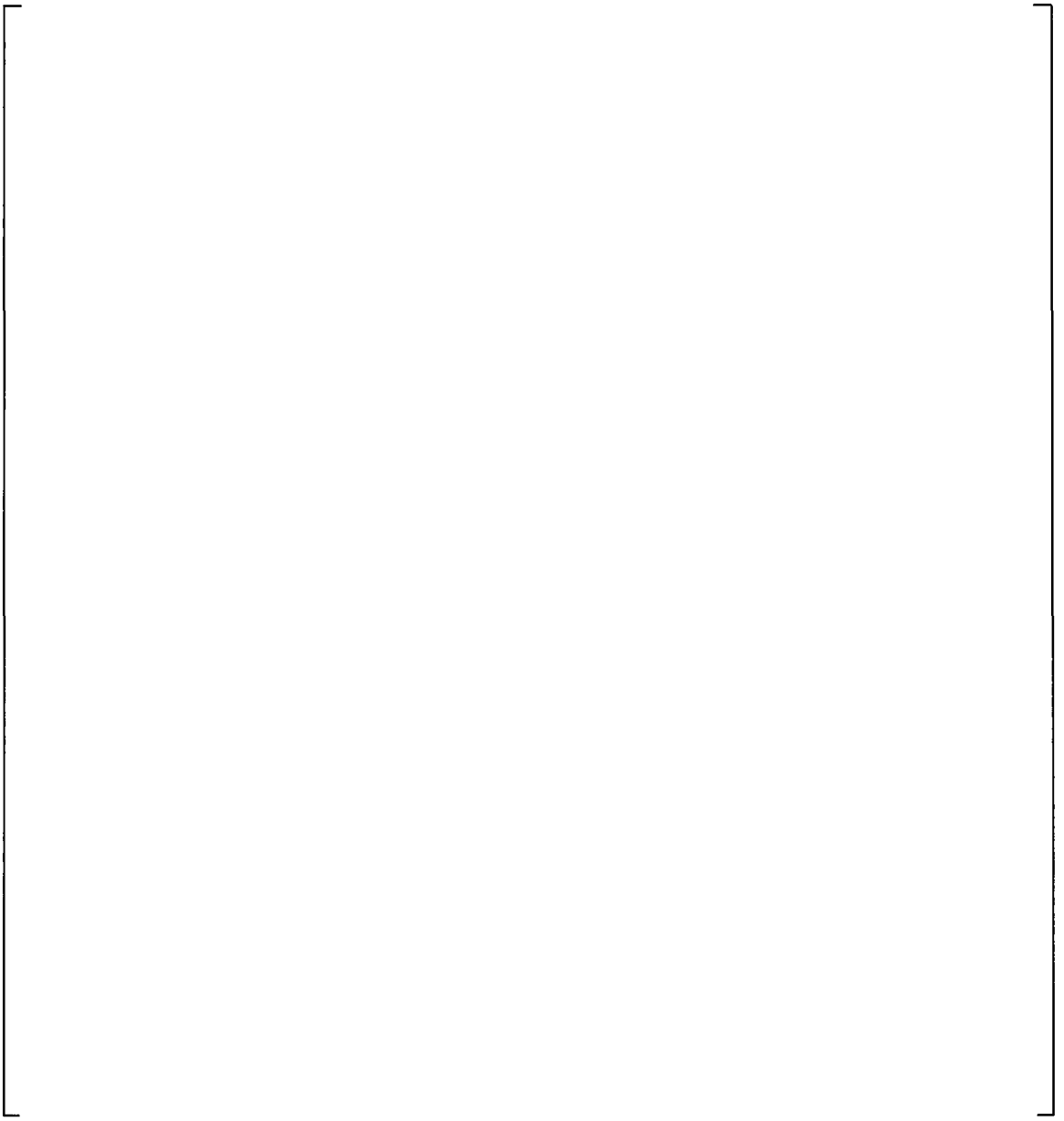

Figure 2-6 Geometry Plot: Dryer Vane-Bank Region

a,c

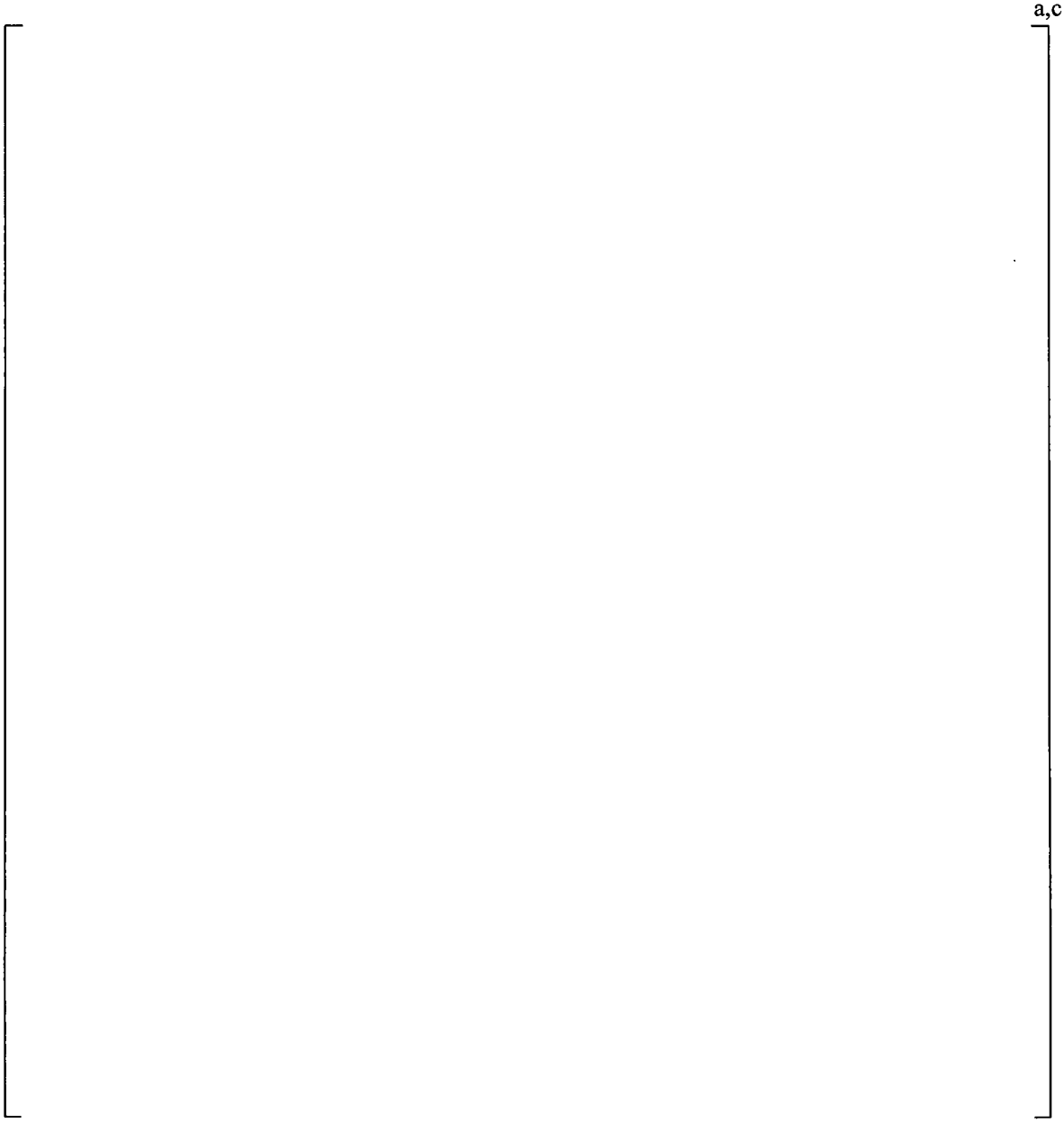

Figure 2-7 Geometry Plot: [ ]a,c

a,c

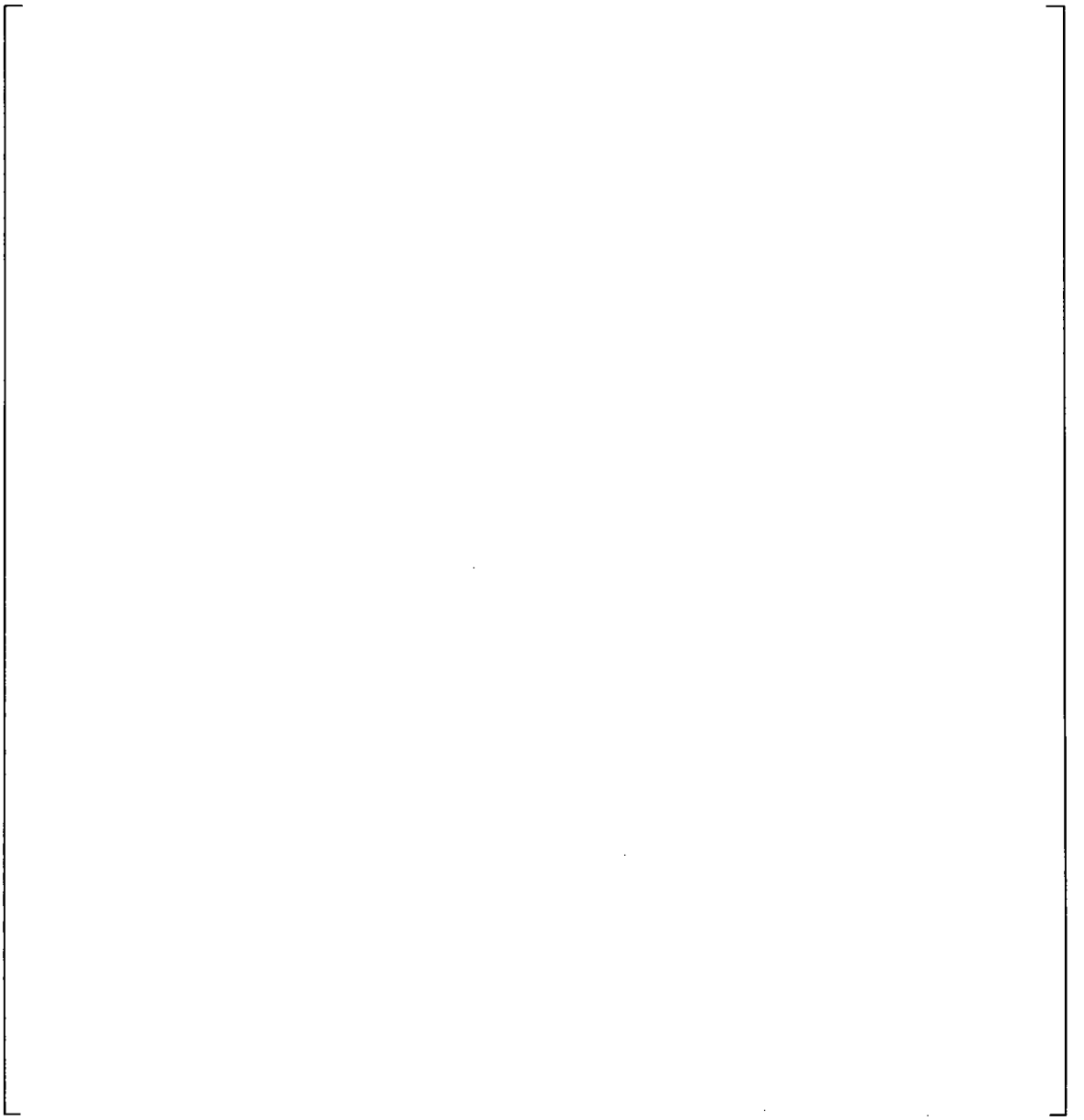

Figure 2-8 Geometry Plot: [ ]a,c

3 FINITE ELEMENT MODEL DESCRIPTION

3.1 STEAM DRYER GEOMETRY

The Monticello replacement steam dryer FEM, generated using the ANSYS® computer code[1], is shown in Figure 3-1. The model consists primarily of [

]^{a,c}.

[

]^{a,c}.

The dryer structure includes [

]^{a,c}.

The [

-
-
-]^{a,c}

Figure 3-11 shows the lifting rod arrangement. Figure 3-12 and Figure 3-13 show details of the hood mesh. Note that the different colors in all of the figures represent different dryer components based on either plate thickness or function. These components can be selected for individual post processing.

[1] The analysis qualification of the Monticello replacement steam dryer was performed using the ANSYS computer code, Release 11, Service Pack 1.

3.2 FINITE ELEMENT MODEL MESH AND CONNECTIVITY

The dryer plates are all modeled [

]^{a,c}.

The vane bank [

]^{a,c}.

[

]^{a,c} are shown in Figure 3-16.

3.2.1 Vane-Bank Representation

The vane bank modules are box-like structures with many internal hanging chevrons. [

]^{a,c} and are shown in more detail in Figure 3-17.

The perforated plates [

]^{a,c} are shown in Figure 3-18.

Also shown in Figure 3-18 are the [

]^{a,c}.

The vane bank [

]^{a,c} are shown in Figure 3-14.

3.2.2 Lifting Rod Representation

The lifting rod is modeled [

]^{a,c} are shown in Figure 3-16.

3.2.3 Dryer Skirt Submerged in Water

The dryer skirt is partially submerged in water. The skirt and drain channel components are separated into groups above and below the water line. The acoustic loading is only applied to elements above the water line. The material density for the stainless steel below water has been adjusted to account for the effect of the hydrodynamic mass.

a,c

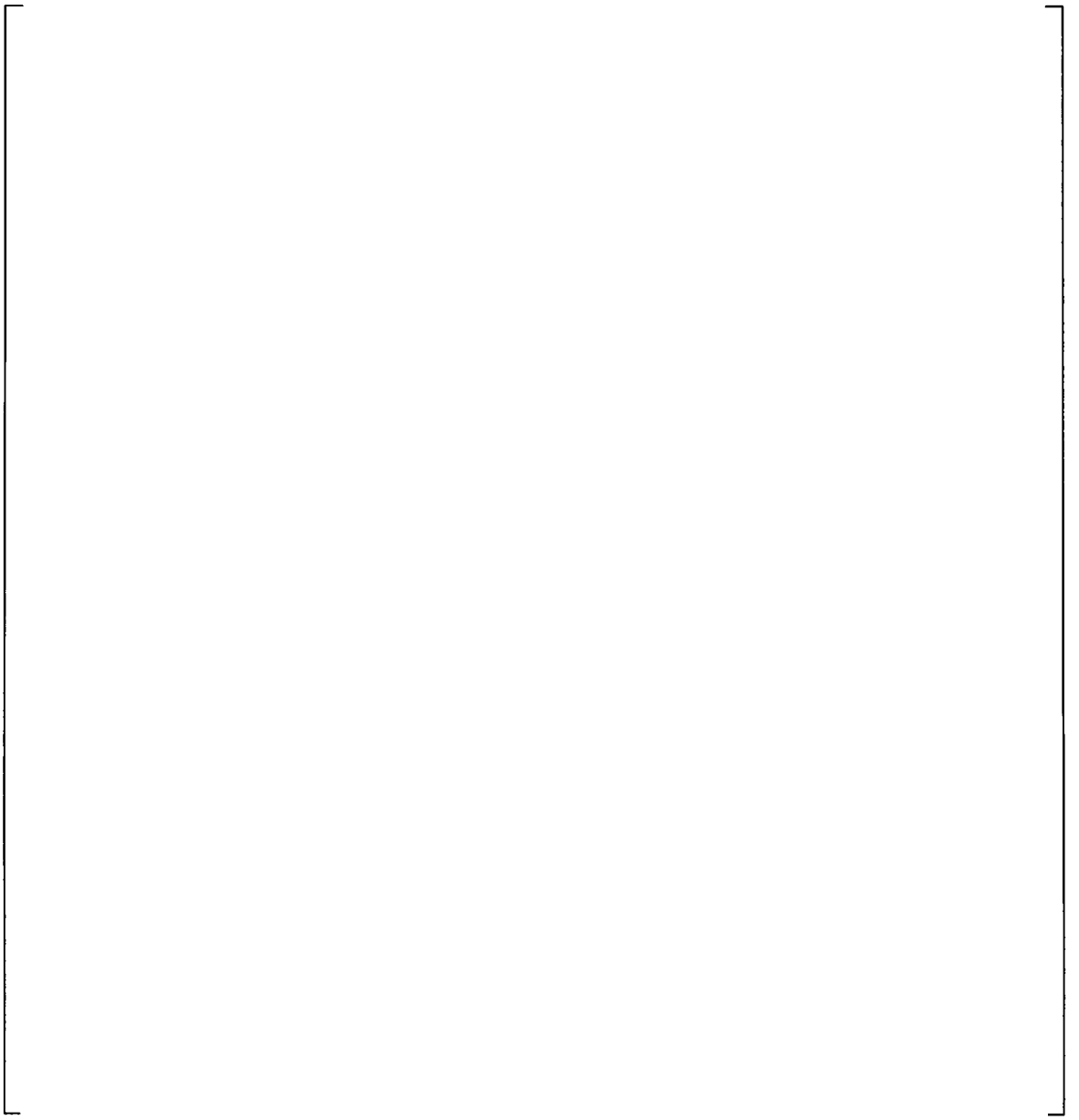

Figure 3-1 Overall Geometry of the Monticello Replacement Steam Dryer Model

a,c

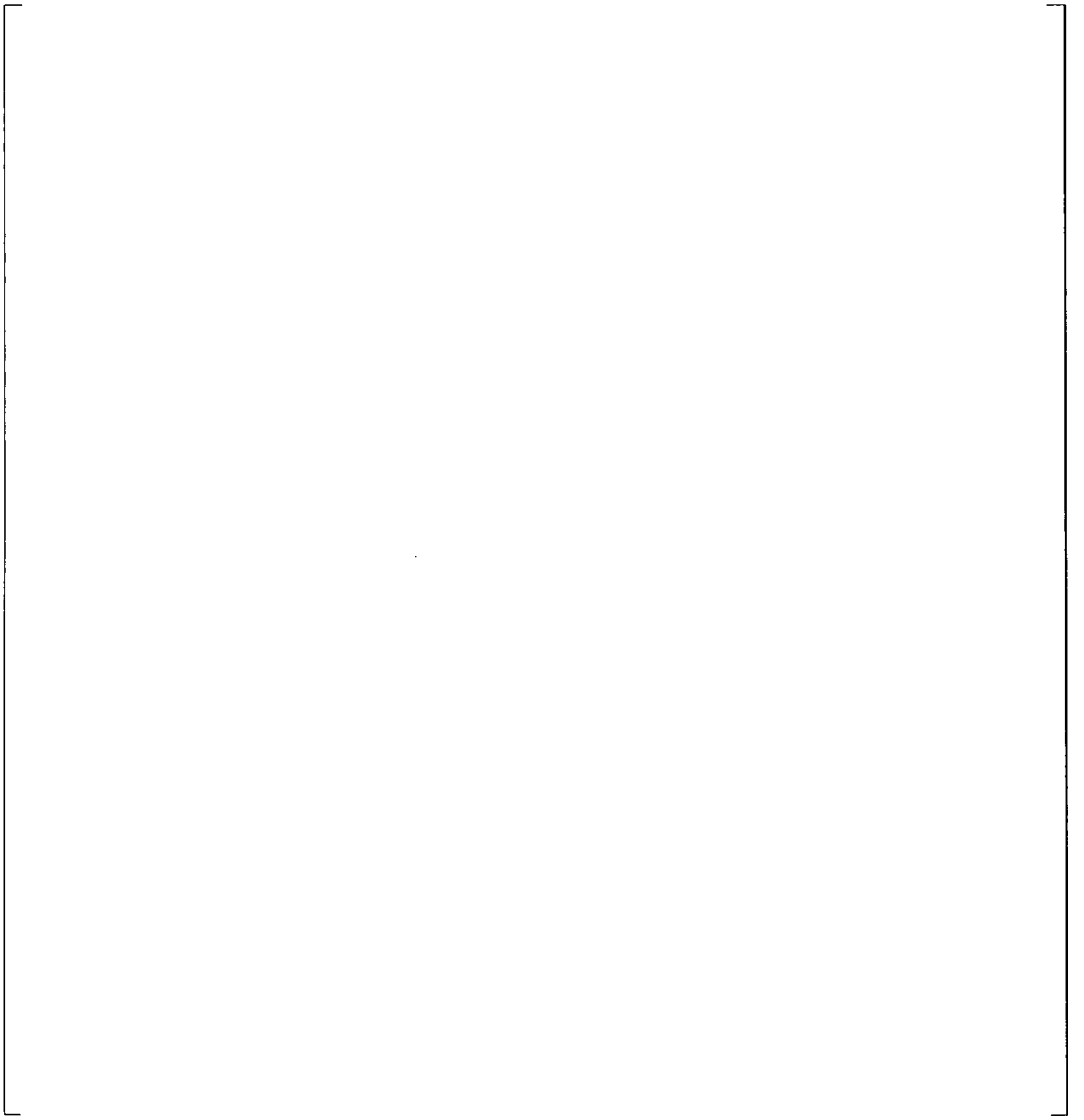

Figure 3-2 Lower [ ]^{a,c}

a,c

[

]

Figure 3-3 Lower [ ]^{a,c}

a,c

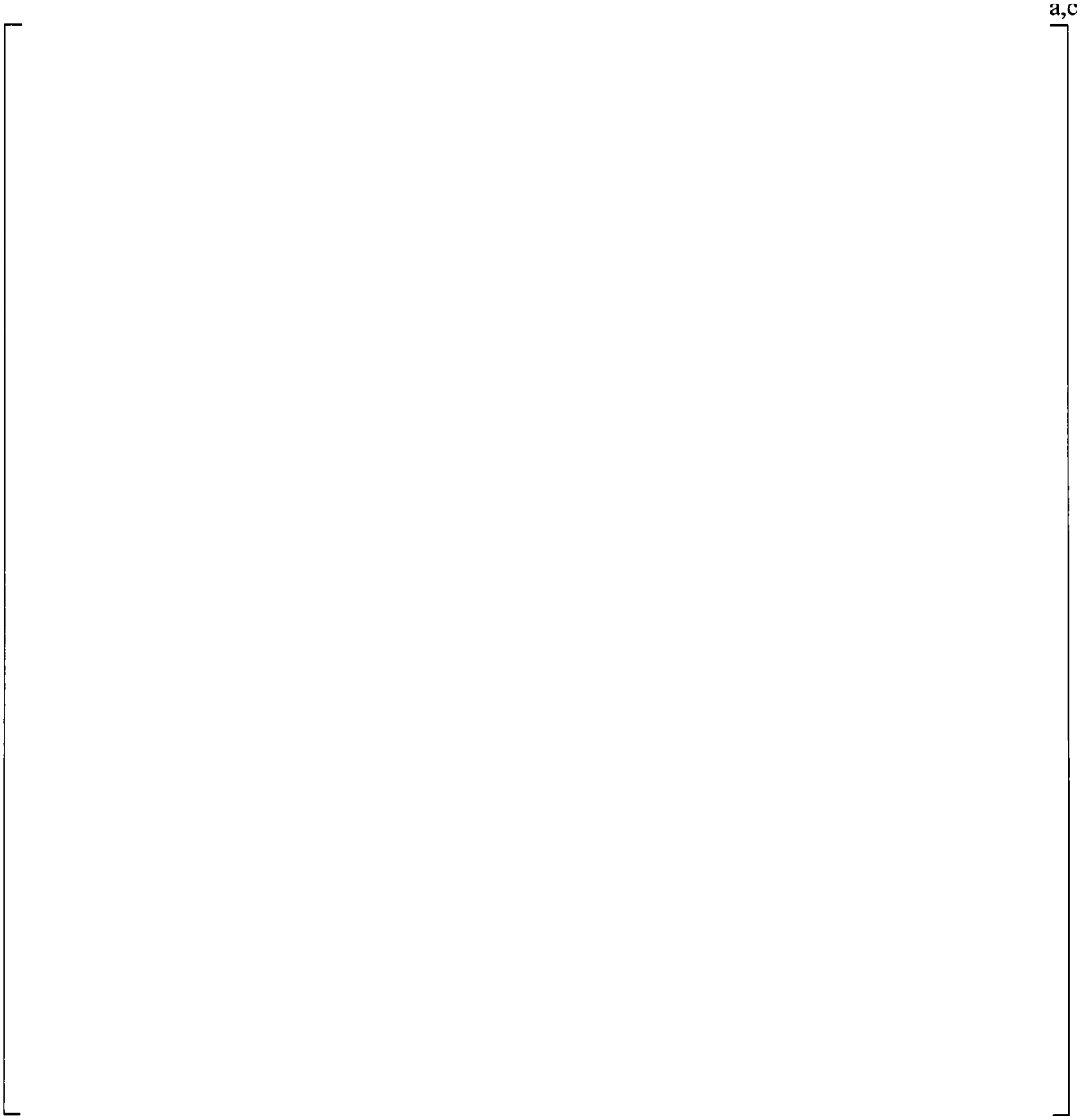

Figure 3-4 Vane-Bank Structural Components

a,c

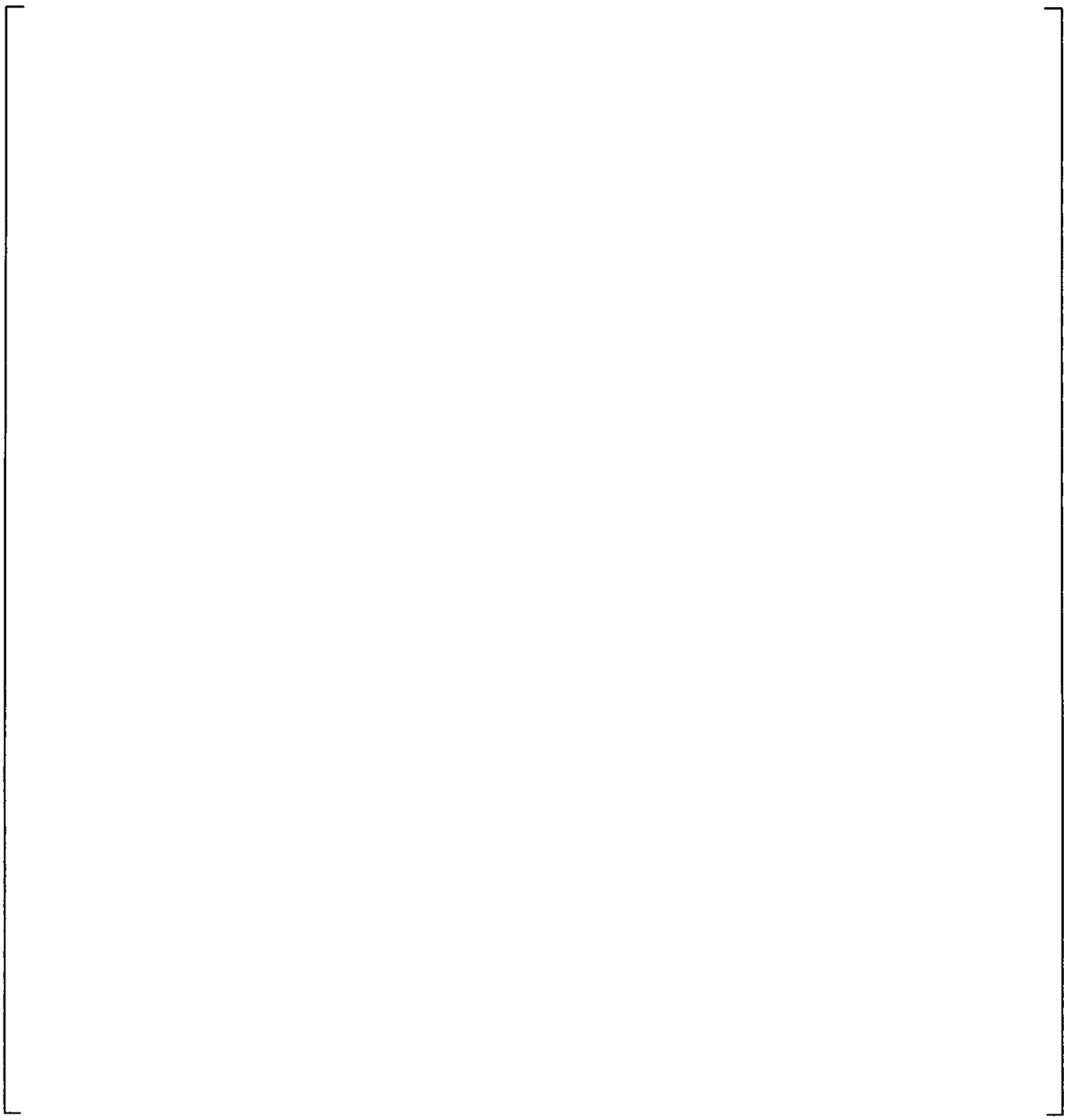

Figure 3-5 Vane-Bank Geometry

a,c

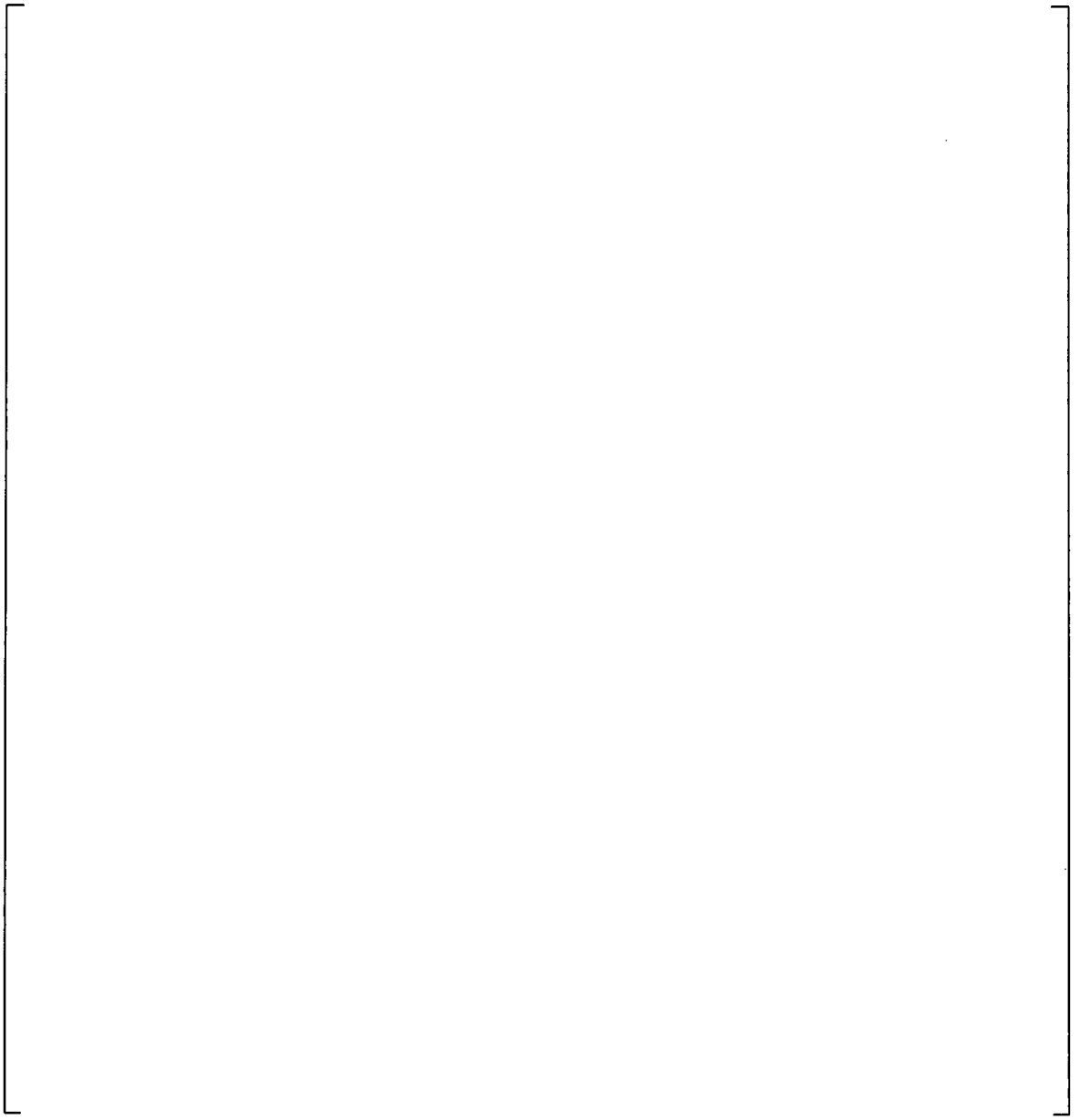

Figure 3-6 Dryer Hood Geometry

a,c

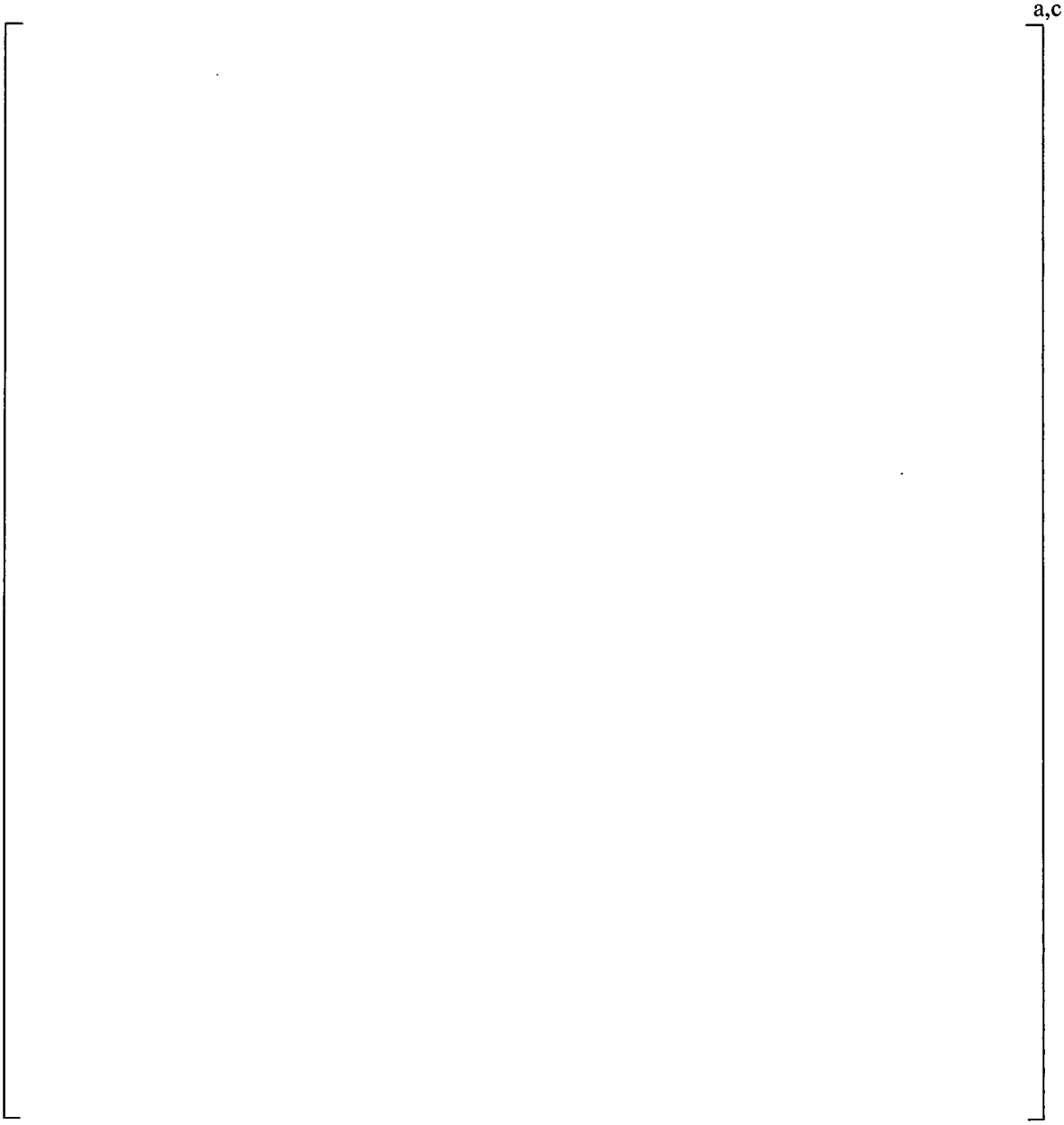

Figure 3-7 Skirt Geometry

a,c

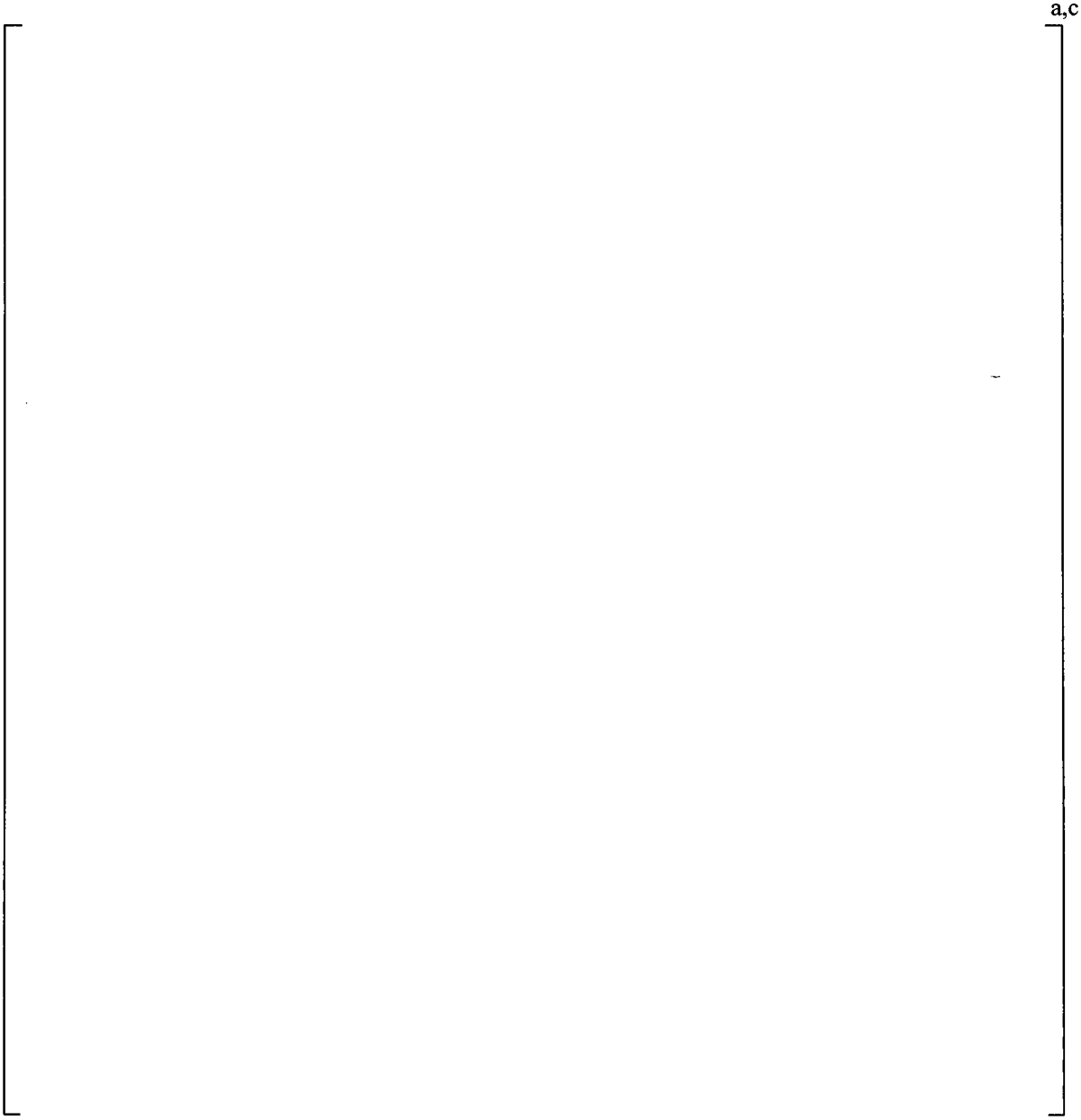

Figure 3-8 [ ]a,c

a,c

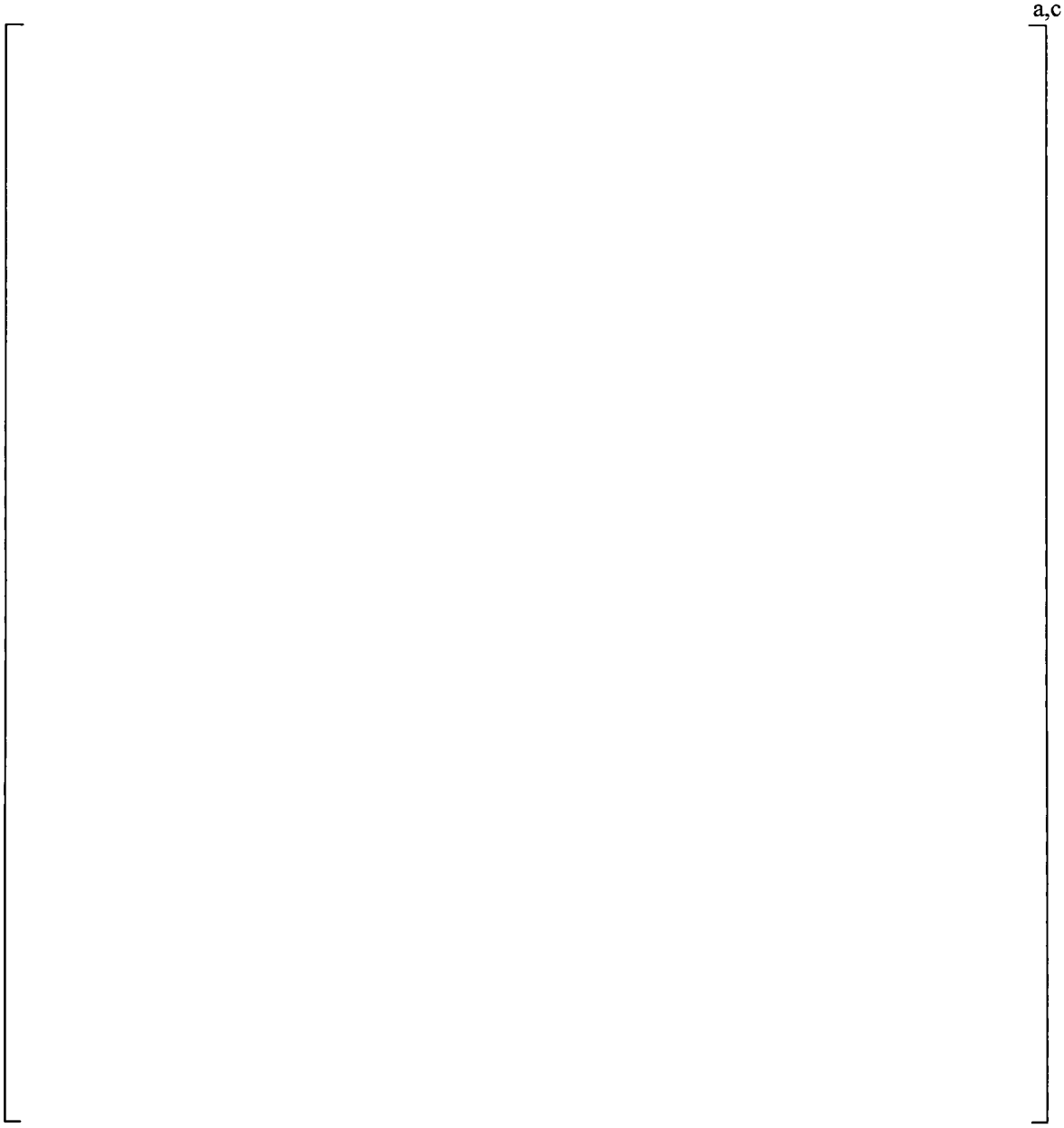

Figure 3-9 [ ][a, c]

a,c

[

]

Figure 3-10 [ ]^{a,c}

a,c

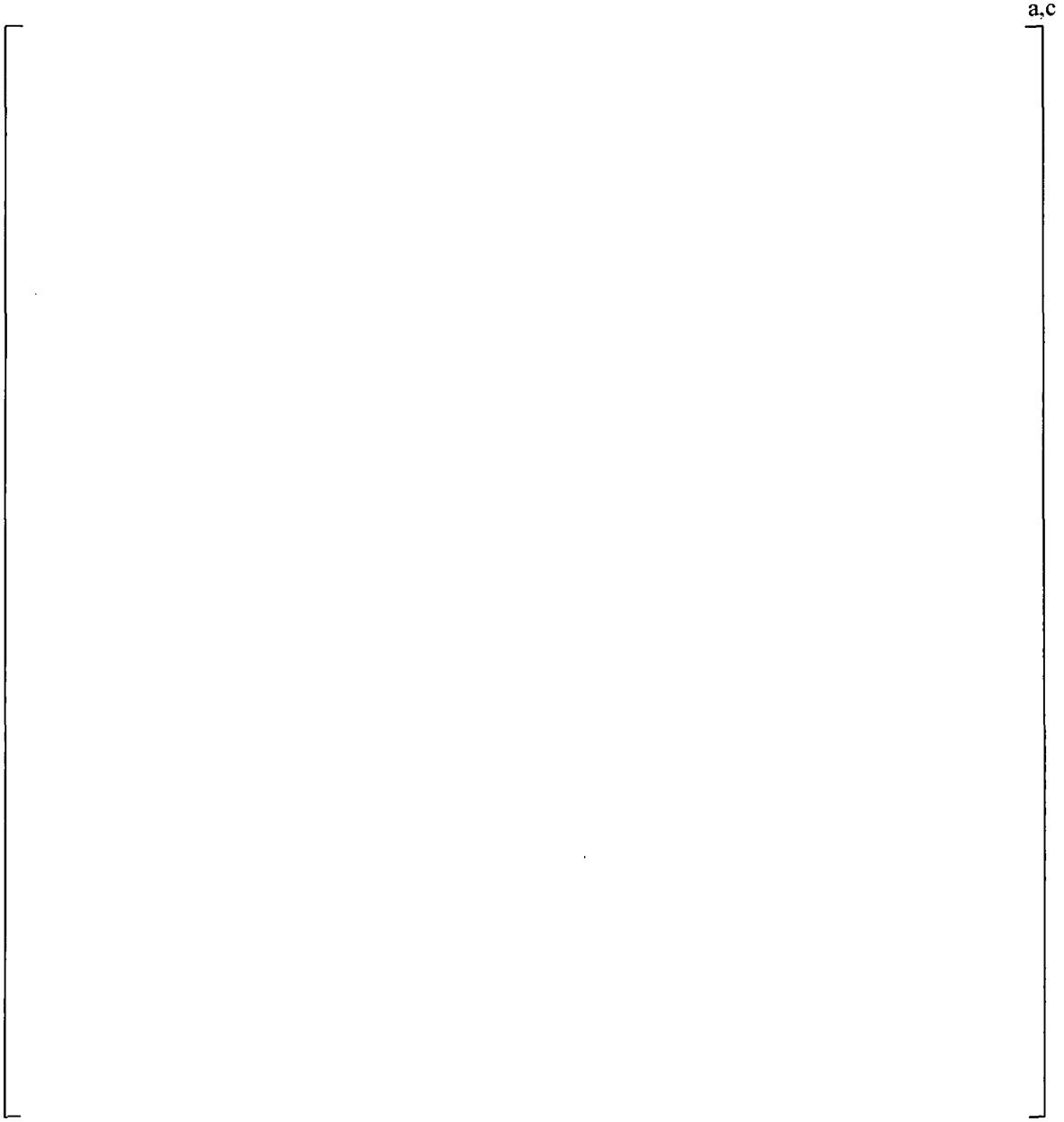

Figure 3-11 Lifting Rod Geometry

a,c

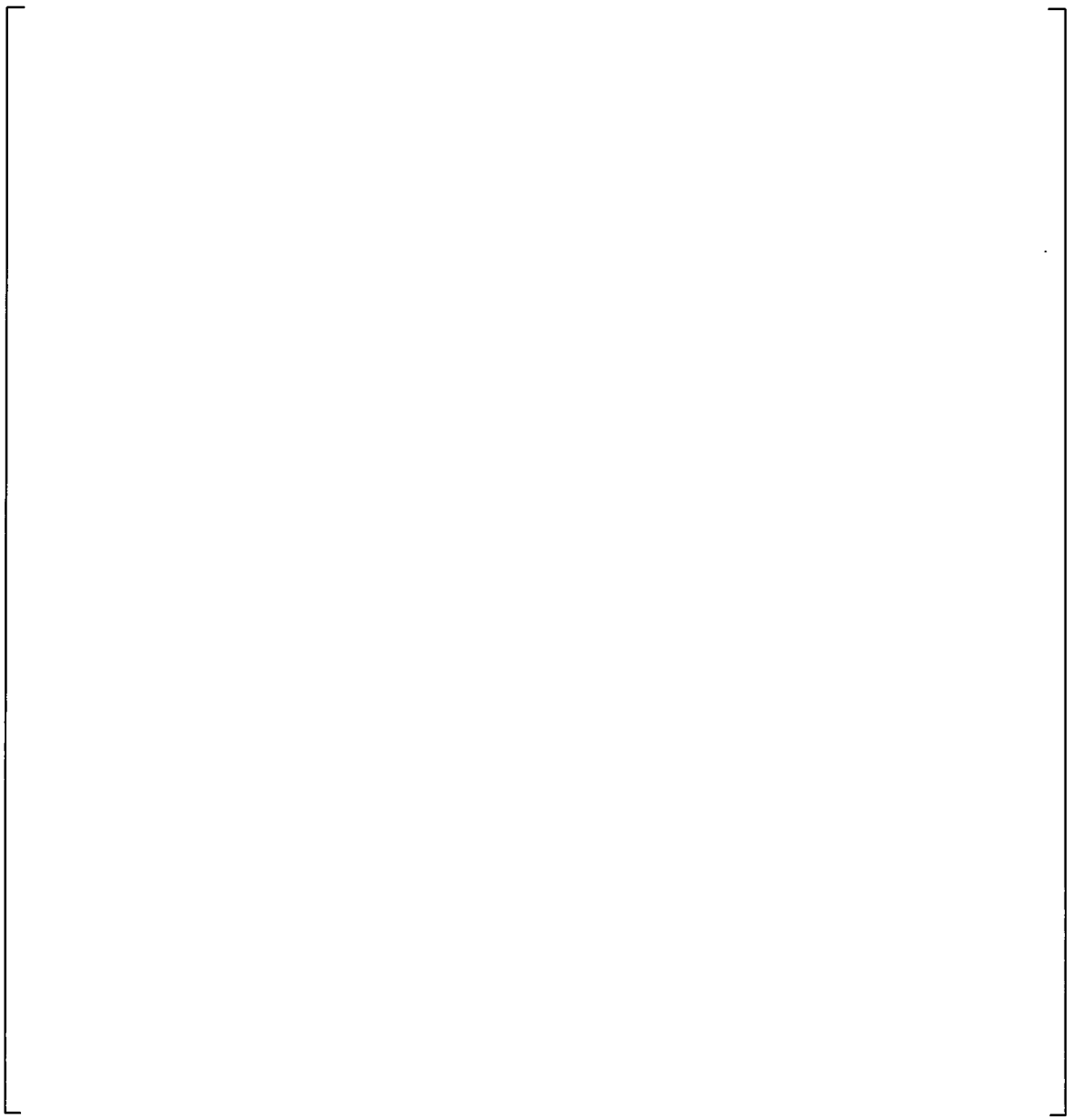

Figure 3-12 [ ][a, c]

a,c

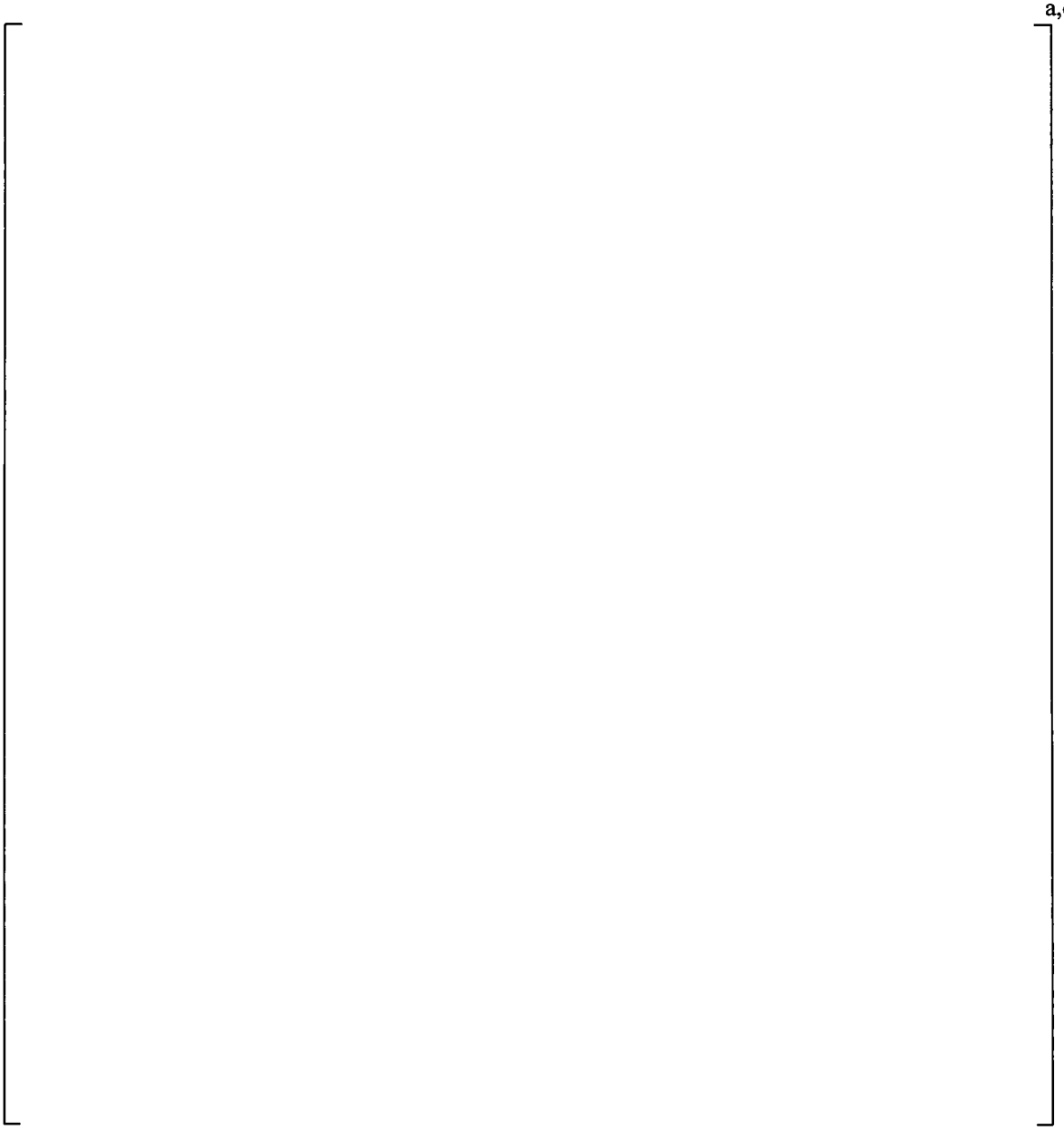

Figure 3-13 [ ]a,c

a,c

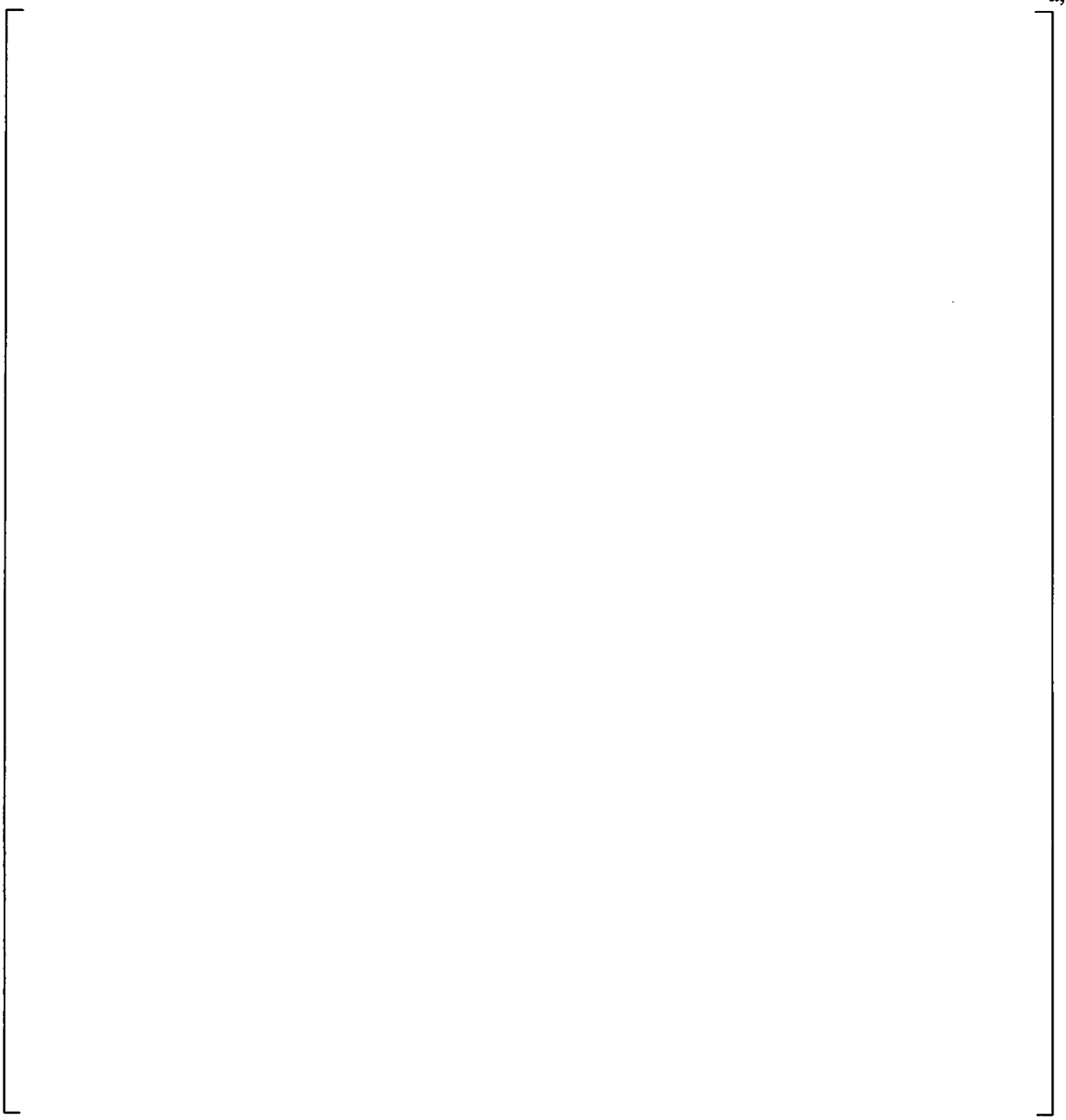

Figure 3-14 [**]**[a, c]**

a,c

[

]

Figure 3-15 [ ][a, c]

a,c

[

]

Figure 3-16 [ ][a,c]

a,c

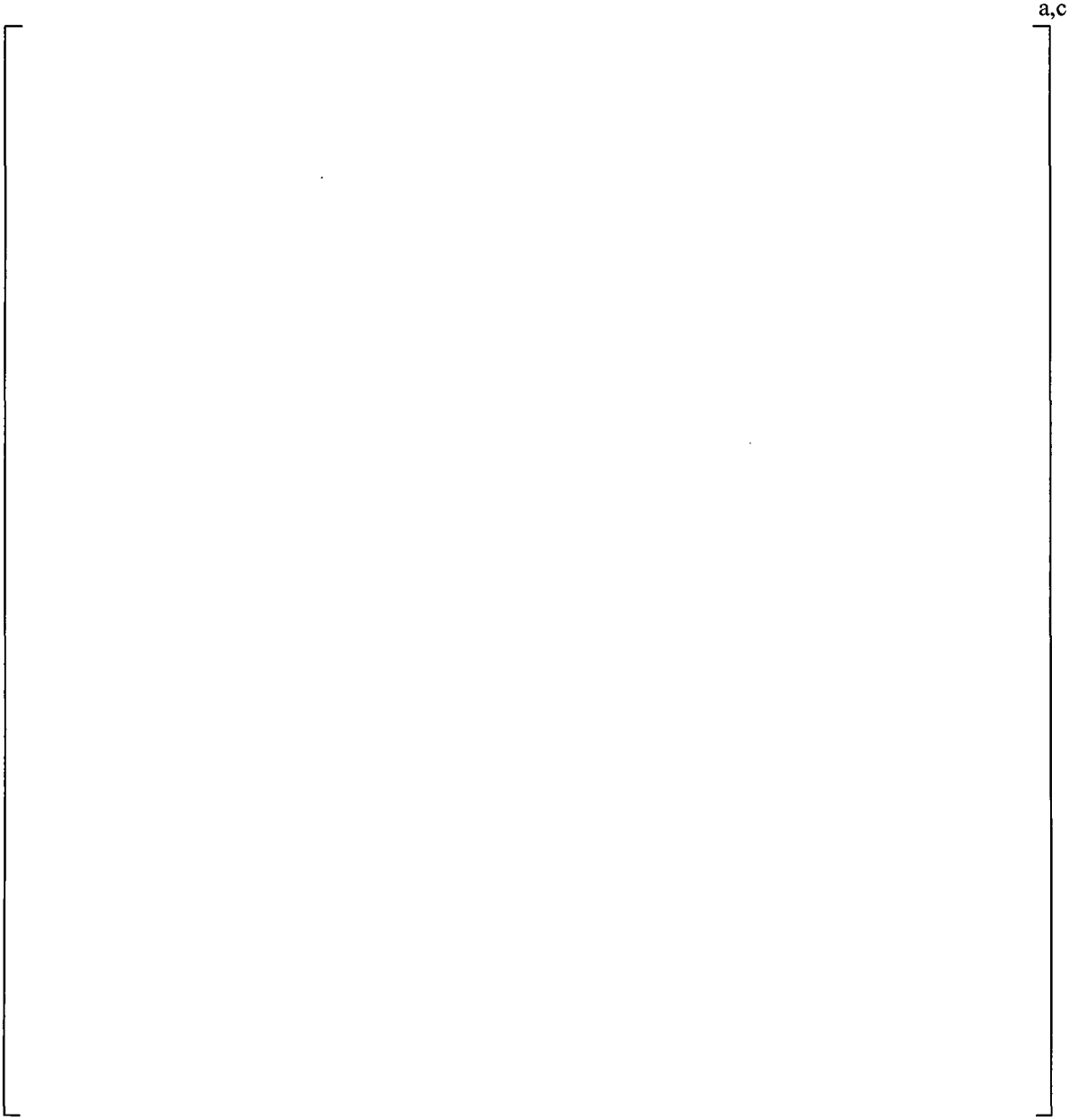

Figure 3-17 Structural Components of Vane Bank

a,c

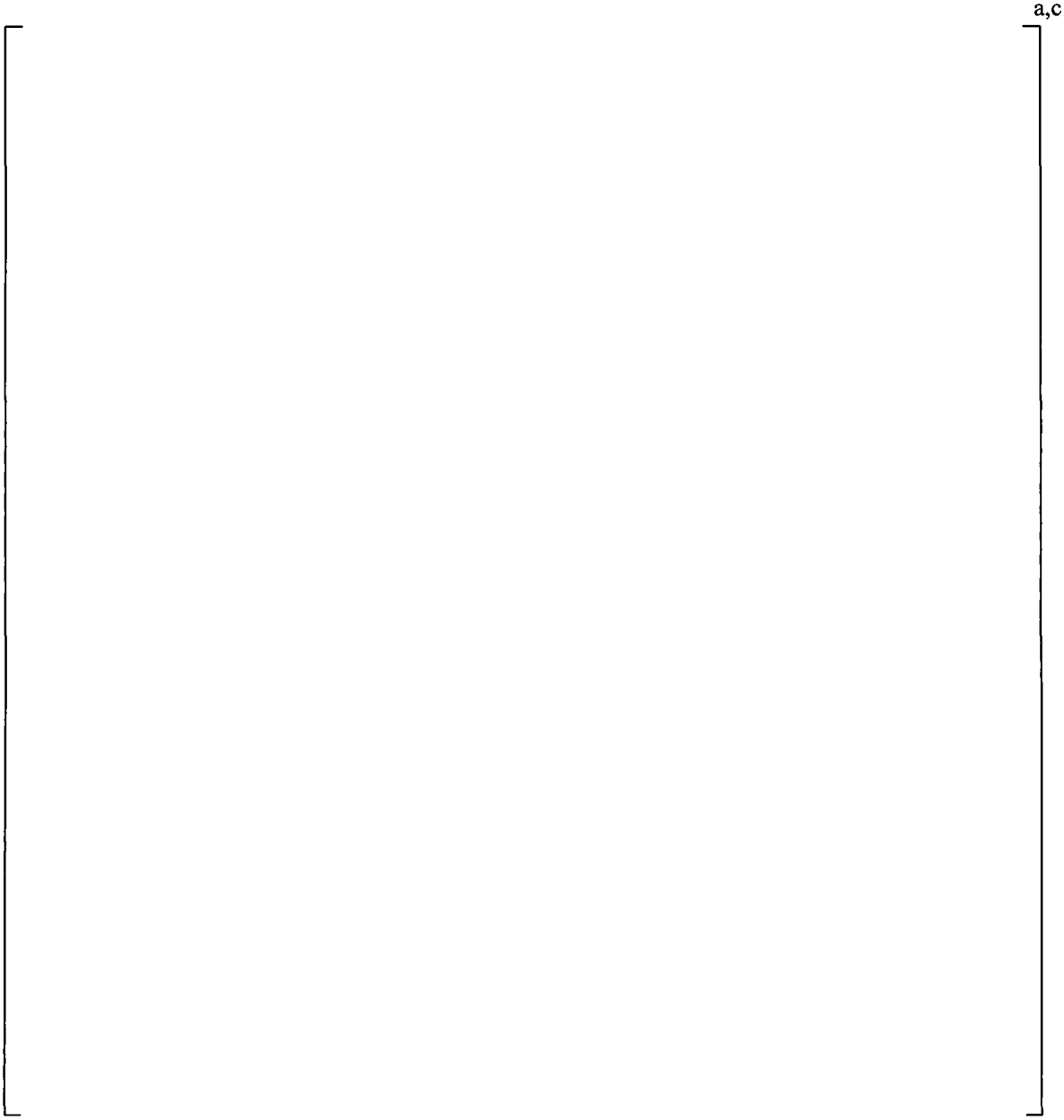

Figure 3-18 Non-Structural Components of Vane Bank

a,c

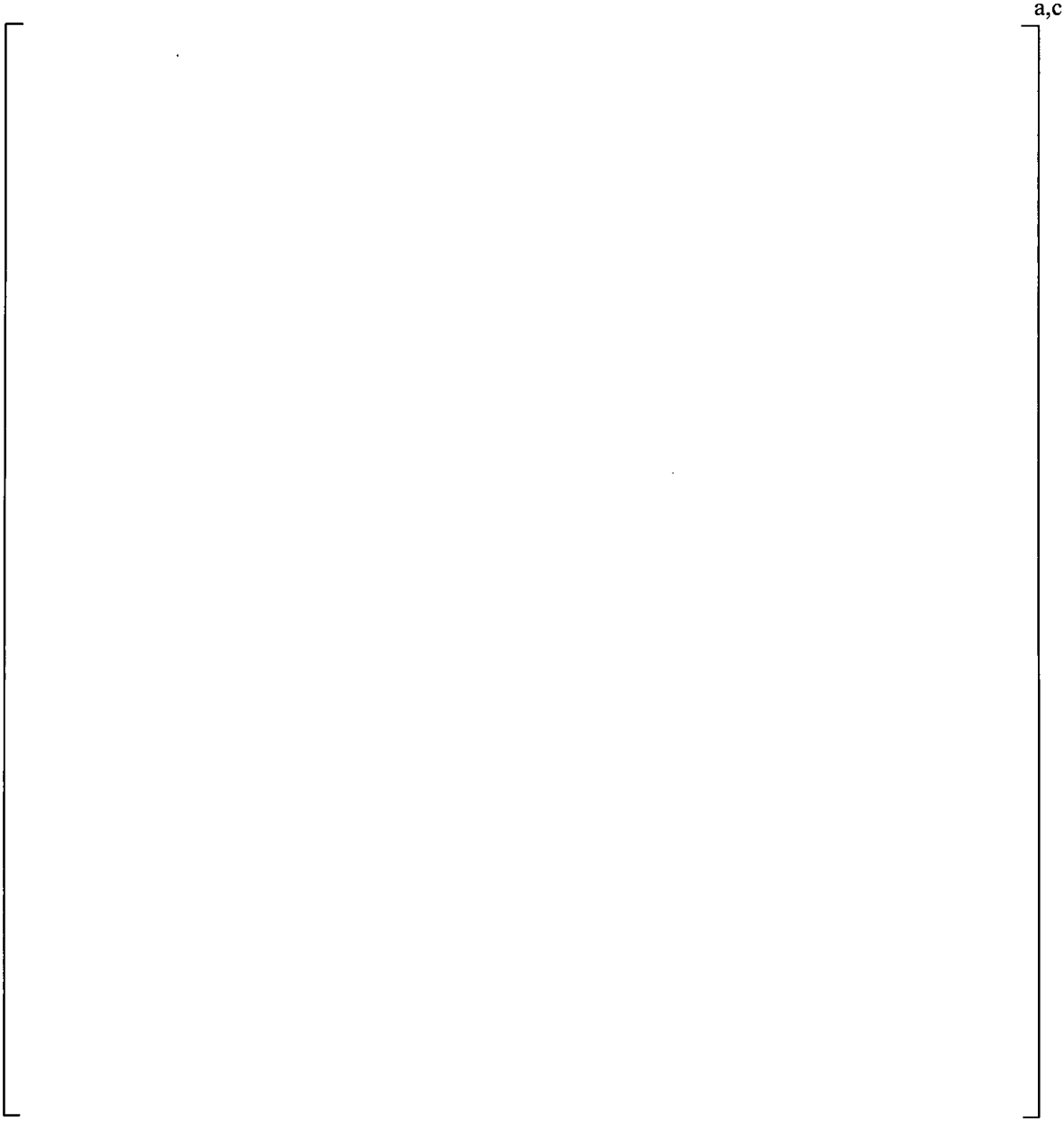

Figure 3-19 Vane-Bank Mass Blocks

a,c

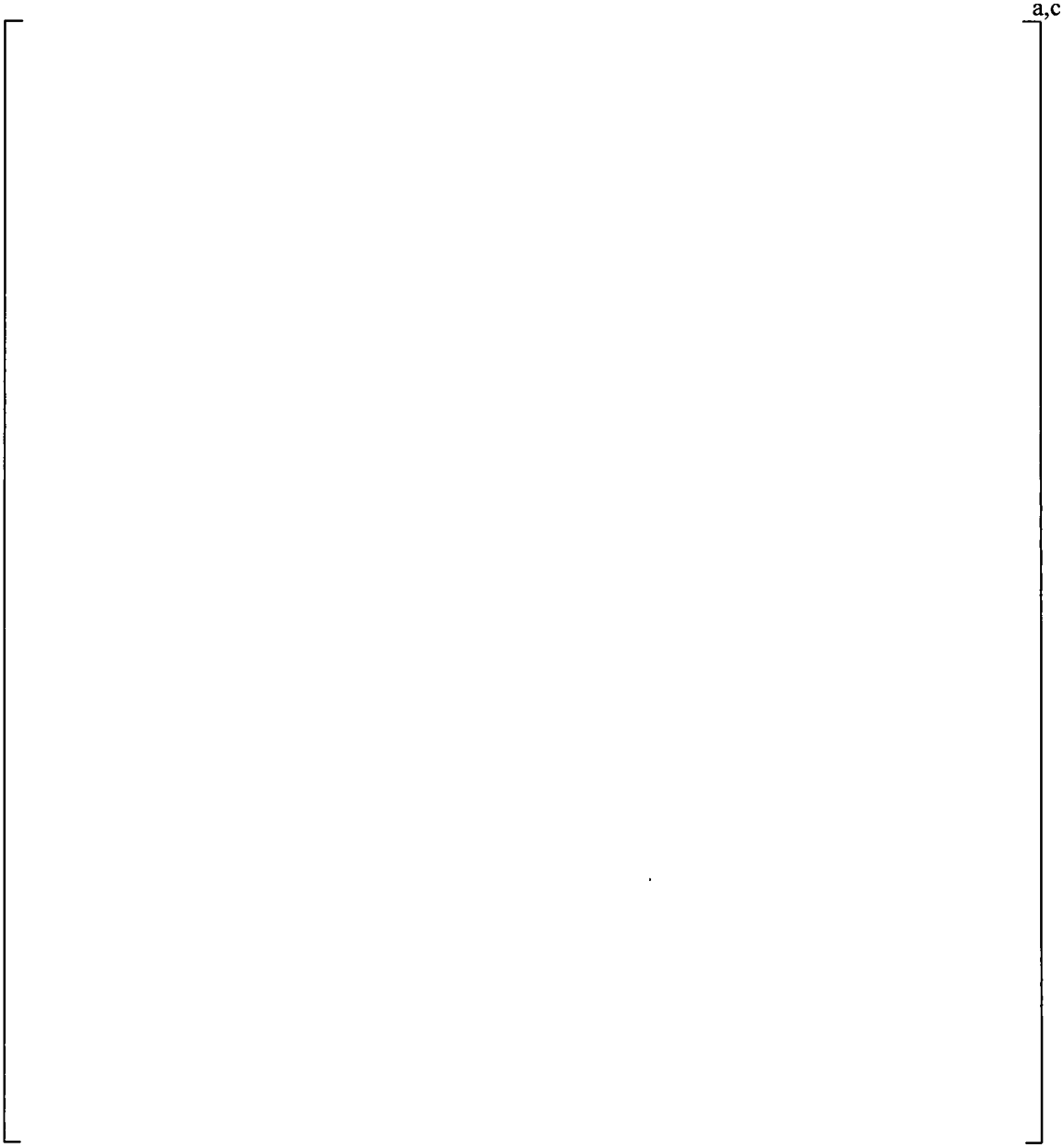

Figure 3-20 Tie Rod Connection between Mass Blocks and End Plates

4 MATERIAL PROPERTIES

A summary of the material properties used in the structural analysis is summarized in Table 4-1. Material properties are taken from the ASME Code, Reference 4, for SS316L at a temperature of 575°F. The density of the skirt material below the water is increased to account for hydrodynamic effects of the water. The perforated plates, located at the entrance to the vane banks, are modeled with equivalent plate properties to account for the reduced stiffness and mass of the plates. The density of the solid block representation of the vane banks is adjusted to achieve the correct overall mass of each vane bank.

4.1 STRUCTURAL DAMPING

Structural damping is defined as 1% of critical damping for all frequencies. This damping is consistent with guidance given on page 10 of NRC RG-1.20 (Reference 5). Using the harmonic analysis approach, a consistent damping level is used across the frequency domain.

Table 4-1 Summary of Material Properties

a,b,c

5 MODAL ANALYSIS

As a precursor to performing the transient analysis, a modal analysis of the dryer was performed. The modal analysis was performed for modes between 0 Hz and 140 Hz. The fundamental modes for the hood and skirt are shown in Figure 5-1 through Figure 5-8. The fundamental modes for the [ ]^{a,c}, respectively.

a,c

Figure 5-1 Modal Analysis: [ ][a,c]

a,c

Figure 5-2 Modal Analysis: [ ]a,c

a,c

Figure 5-3 Modal Analysis: [ ][a,c]

a,c

Figure 5-4 Modal Analysis: [ ]a,c

a,c

Figure 5-5 Modal Analysis: [ ]a,c

a,c

Figure 5-6 Modal Analysis: [ ][a,c]

a,c

Figure 5-7 Modal Analysis: [ ]a,c

a,c

Figure 5-8 Modal Analysis: [ ]a,c

6 LOAD APPLICATION

The frequency-dependent acoustic loads were developed using a three-dimensional (3-D) acoustic model representation of the dryer assembly. The acoustic pressure (P) loads on the steam dryer structure were calculated by [

]^{a,c}.

[

]^{a,c}

a,c

Figure 6-1 Helmholtz Acoustic Model

a,c

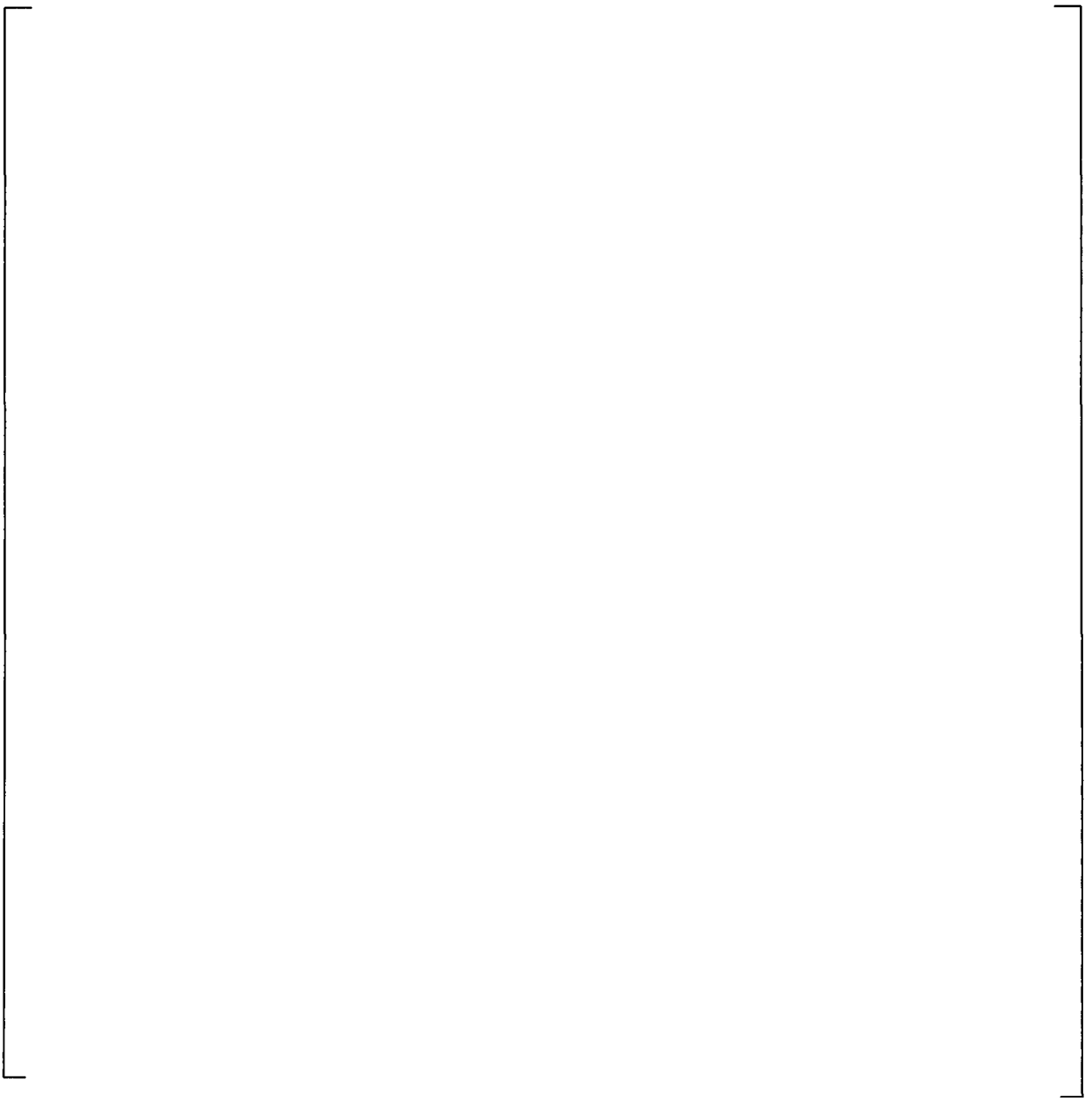

Figure 6-2 Three-Dimensional Views of the Acoustic Model

a,c

Figure 6-3 ACE and FEM Global Coordinate System Layout, Top View

a,c

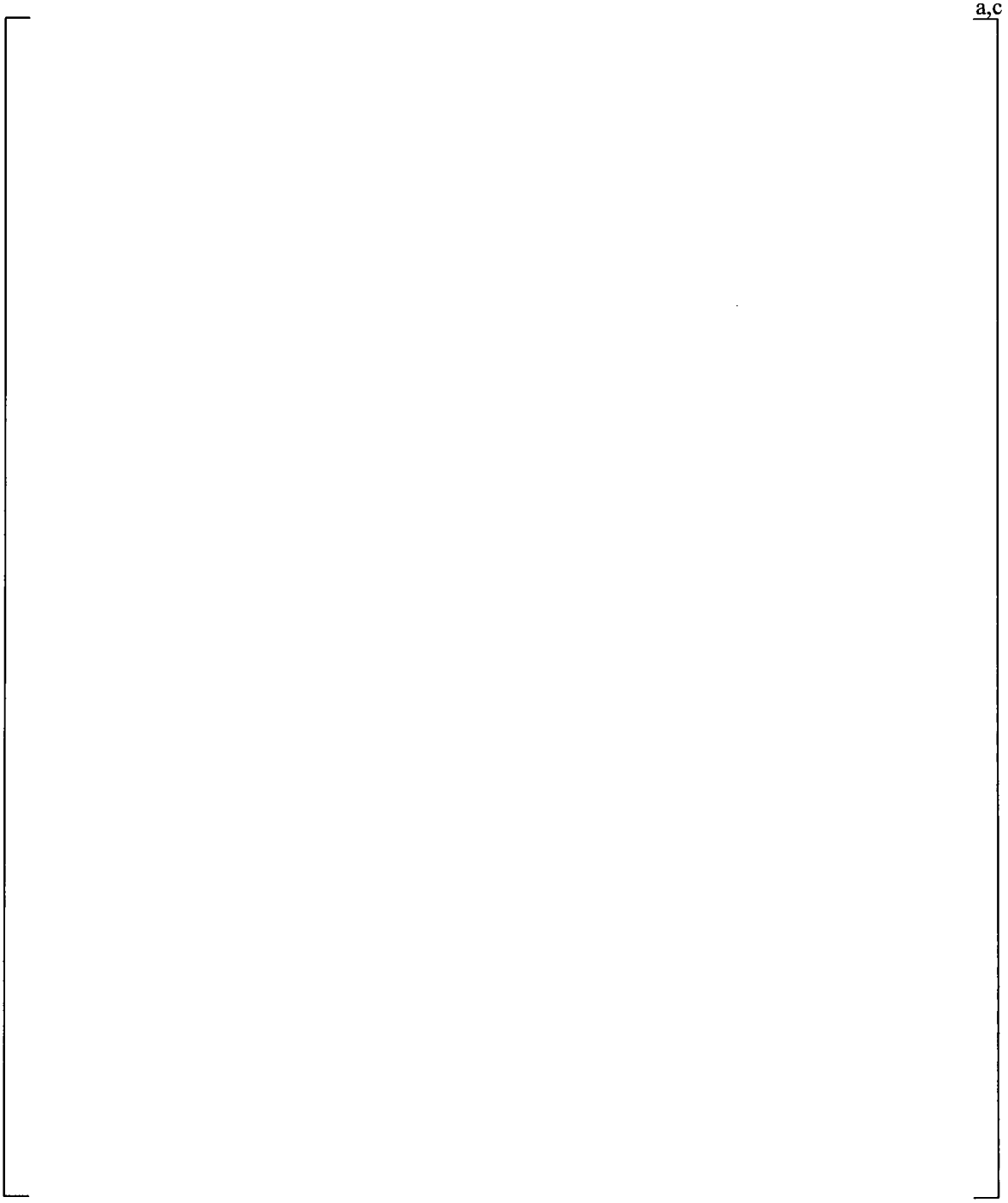

Figure 6-4 ACE and FEM Global Coordinate System Layout, Section View

7 STRUCTURAL ANALYSIS

7.1 HARMONIC ANALYSIS

7.1.1 [ ]^{c}

Harmonic solutions are obtained using the ANSYS FEM for the following sets of conditions.

- **Model Support (Boundary) Conditions**

  The model is supported [

  ]^{a,c}.

- **Operating Conditions**

  98% of CLTP and 100% of EPU operating conditions are evaluated.

- **Frequency Shifts**

  [

  ]^{a,c}.

7.1.2 Overview – Time-History Solution

The harmonic analysis begins with the [

]^{a,c}. As discussed above, separate solutions are obtained for [

]^{a,c}.

[

]^{a,c}.

[

]^{a,c}.

It is inefficient to process the results [

]^{a,c}.

[

]^{a,c}.

[

]^{a,c}.

7.1.3 Inverse Fourier Transform

[

]^{a,c}.

7.1.4 Frequency Scaling (Shifting)

As a result of approximations of the structural interactions used in developing the FEM, small errors can result in the prediction of the component natural frequencies. Varying degrees of mesh discretization can also introduce small errors in the FEM results. To account for these effects, frequency scaling is applied to the applied load-history.

If frequency scaling is applied, [

]^{a,c}

7.2 POST-PROCESSING

7.2.1 Primary Stress Evaluation

Once the time-history has been calculated [ ]^{a,c}, an evaluation is performed to calculate the maximum alternating stress intensity. The stress intensities for the [

]^{a,c}.

For a 2-D stress field, the principal stresses are calculated as follows (the X-Y plane is used as an example. The same algorithms are also applicable to other planes.)

$$\sigma_{1,2} = \frac{\sigma_x + \sigma_y}{2} \pm \sqrt{\left(\frac{\sigma_x - \sigma_y}{2}\right)^2 + \left(\sigma_{xy}{}^2\right)}$$

$$\sigma_3 = 0.0$$

$$\text{Stress Intensity} = \text{Maximum} \begin{matrix} |\sigma_1 - \sigma_2| \\ |\sigma_2 - \sigma_3| \\ |\sigma_3 - \sigma_1| \end{matrix}$$

For a general 3-D state of stress, the resulting principal stresses correspond to the roots of the following cubic equation as:

$$\sigma^3 - a_2\sigma^2 + a_1\sigma - a_0 = 0$$

where,

$$a_2 = \sigma_x + \sigma_y + \sigma_z$$
$$a_1 = \sigma_x\sigma_y + \sigma_y\sigma_z + \sigma_z\sigma_x - \sigma_{xy}{}^2 - \sigma_{yz}{}^2 - \sigma_{zx}{}^2$$
$$a_0 = \sigma_x\sigma_y\sigma_z + 2\sigma_{xy}\sigma_{yz}\sigma_{zx} - \sigma_x\sigma_{yz}{}^2 - \sigma_y\sigma_{zx}{}^2 - \sigma_z\sigma_{xy}{}^2$$

7.2.2 Alternating Stress

The calculation of the alternating stress intensity, following the ASME Code process, is performed as follows.

1. Apply the SCFs (geometric or fatigue strength reduction factor (FSRF)), as applicable, to the component stresses.

2. Calculate the range of stress for each component of stress for two time points.

3. Calculate the stress intensity of the component ranges.

[

]^{a,c}.

7.3 CALCULATING AND EVALUATING WELD STRESSES

Due to the nature of the dynamic analysis, detailed modeling of the welds is not practical in the global dryer FEM. Calculating weld stresses requires a different approach. For the Monticello replacement steam dryer, [

]^{a,c}.

7.3.1 Detailed Fillet Weld Calculations

As discussed above, detailed weld stresses are not directly available from the finite element analysis.
[

]^{a,c}.

[

]^{a,c}.

7.3.2 Calculating and Evaluating Weld Stresses [ ]^{a,c}

For the full penetration welds, [

]^{a,c}.

7.4 [ ]^{a,c}

[

]^{a,c}.

[a,c

]

Figure 7-1 [ ]^{a,c}

8 ANALYSIS RESULTS

8.1 GLOBAL MODEL

As discussed previously, [

]^{a,c}.

A summary [

]^{a,c}

8.2 [ ]^{a,c}

8.2.1 [ ]^{a,c}

[

]^{a,c}.

8.3 [ ]^{a,c}

8.3.1 [ ]^{a,c}

[

]^{a,c}

Table 8-1 Stress Results for 98% of CLTP Conditions

a,b,c

Table 8-1 (cont.) Stress Results for 98% of CLTP Conditions

a,b,c

Table 8-2 Stress Results for EPU Conditions

a,b,c

Table 8-2 (cont.) Stress Results for EPU Conditions

a,b,c

Table 8-3 [ ]^{a,c} for 98% of CLTP

a,b,c

Table 8-4 [ ]^{a,c} for EPU

a,b,c

a,c

Figure 8-1 [ ][a,c]

9 SUMMARY OF RESULTS AND CONCLUSIONS

[

]^{a,c}.

Table 9-1 Summary of Results: 98% of CLTP Conditions

a,b,c

Table 9-2 Summary of Results: EPU Conditions

a,b,c

10 REFERENCES

1. Westinghouse Electric Sweden AB Report SES 09-127, Rev. 2, *Monticello Steam Dryer Replacement – Structural Verification of Steam Dryer*, June 2010. (Westinghouse Proprietary)

2. *ASME Boiler and Pressure Vessel Code,* 2004 Edition, Section III, Division 1.

3. BWRVIP-182-A, *Guidance for Demonstration of Steam Dryer Integrity for Power Uprate*, Electric Power Research Institute, Palo Alto, CA, May 2010.

4. *ASME Boiler and Pressure Vessel Code*, 2004 Edition, Section II, Part D.

5. U.S. Nuclear Regulatory Commission, Regulatory Guide 1.20, Rev. 3, *Comprehensive Vibration Assessment Program for Reactor Internals During Preoperational and Initial Startup Testing*, March 2007.

6. Westinghouse WCAP-17251-P, Rev. 0, "Monticello Replacement Steam Dryer Four-Line Acoustic Subscale Testing Report," June 2010. (Westinghouse Proprietary)

7. Westinghouse WCAP-17252-P, Rev. 2-A, *Acoustic Loads Definition for the Monticello Steam Dryer Replacement Project*, March 2012. (Westinghouse Proprietary)

8. Westinghouse WCAP-17540-P, Rev. 0-A, *Monticello Replacement Steam Dryer Program Acoustic Load Definition Methodology*, March 2012. (Westinghouse Proprietary)

9. [

]^{a,c}.

ENCLOSURE 13

NON-PROPRIETARY ATTACHMENT FROM WESTINGHOUSE LETTER LTR-A&SA-09-32, REVISION 5 LIMIT CURVES FOR MONTICELLO POWER ASCENSION

3 pages follow

LTR-A&SA-09-32 NP-Attachment-Revision 5
June 2012

Attachment:
Limit Curves for Monticello Power Ascension

Westinghouse Electric Company LLC
1000 Westinghouse Drive
Cranberry Township, PA 16066 USA

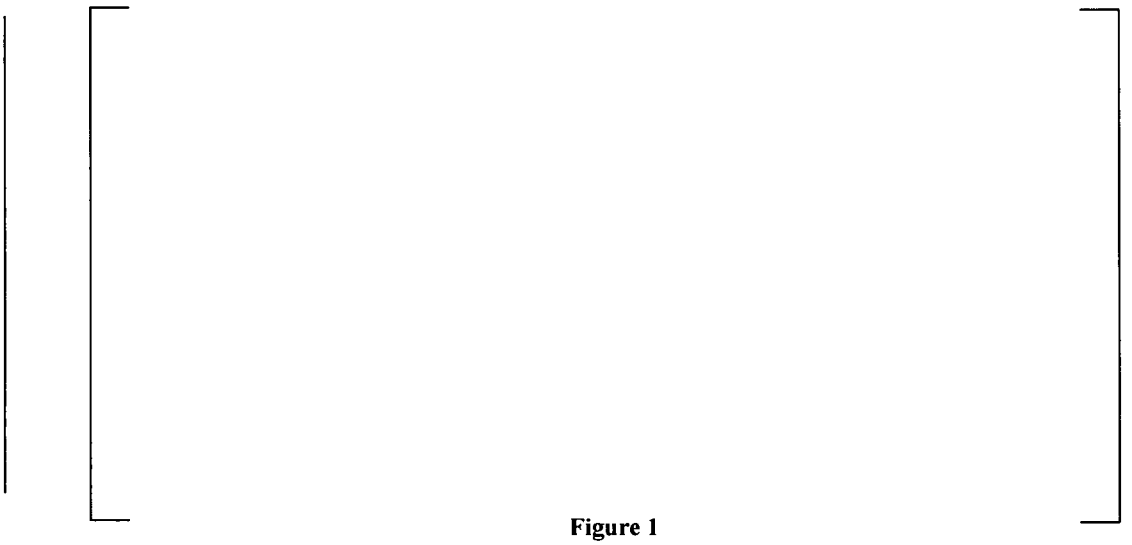

a,c

Figure 1
Limit Curves, MSL A

a,c

Figure 2
Limit Curves, MSL B

a,c

Figure 3
Limit Curves, MSL C

a,c

Figure 4
Limit Curves, MSL D